Chapter III:

Verification and Validation Plan

DRAFT 4/97

1.0 PURPOSE

The goal of the Verification and Validation (V&V) effort is to test the options and features of the FEHM application that satisfy the requirements specified in Chapter I, "Software Requirements Specification." The current chapter, "Verification and Validation Plan," details the test cases to be performed, many of which were developed for prior versions of FEHM (Zyvoloski et al. 1992; Zyvoloski and Dash 1991a and 1991b), and lists the acceptance criteria that must be satisfied.

2.0 FUNCTIONAL DESCRIPTION

The goal of the verification part of the V&V effort is to check the operation of the code for a variety of simulations. These simulations will encompass the options and features of FEHM that will be used in actual simulations of flow and transport in the unsaturated zone and in modeling and interpreting pressure transient tests, temperature logs, and tracer tests (both conservative and reactive tracers) performed in the saturated zone. The overall verification of FEHM will be accomplished by comparison of results with published analytical solutions and with results from other codes. Because of the nonlinear nature of the water and steam properties, additional verification of the thermodynamics package is included. The verification test cases in Section 4.0 of this chapter are organized in groups based on the functions and features being tested and include: testing of the thermodynamic functions (Section 4.1); heat transfer tests (Sections 4.2 and 4.3); isothermal fluid flow tests (Sections 4.4–4.7); combined heat and mass transfer tests (Sections 4.8–4.11); and solute transport tests (Sections 4.12–4.17).

The model-validation part of the V&V effort is in an early stage of development. The goals of validation include modeling of appropriate field tests when experimental data are available from the Yucca Mountain Site Characterization Project. Model validation will not explicitly be discussed in this document but will be included in a later revision when data become available.

3.0 ASSUMPTIONS AND LIMITATIONS

The verification effort assumes that the FEHM application is installed on systems running the UNIX operating system (i.e., Sun Workstations, HP, Cray, IBM, SGI) and that dynamic memory allocation is supported.

When comparing against an analytical solution or other code, it is assumed that close agreement between FEHM and the analytical solution or alternate-model results constitutes a verification of both. Fortuitous agreement between models using entirely different mathematical solution procedures is judged to be extremely unlikely.

The acceptance criteria are based on maximum error, percent error, or root-mean-square (RMS) error. These are standard error measures used in mathematics and the physical sciences. The RMS error indicates average error over the solution domain, and the maximum and percent errors represent the largest errors in the domain. The maximum error is defined to be the absolute value of the maximum difference (error) between the values of the FEHM solution (FS) and the analytical or alternate-model solution (AS), where the error between each point is computed as $Error = abs(AS - FS)$. The percent error (PE) is defined as the error divided by the analytical or alternate-model solution times 100 and is computed for each point using $PE = abs\left(\frac{AS - FS}{AS}\right) \times 100$. The RMS error is calculated using the following: $RMS = \sqrt{\sum\left(\frac{AS - FS}{AS}\right)^2} /$ (Number of points compared).

A relatively new module has been included that simulates solute transport using particle tracking. A series of test cases are being developed but are not yet ready to be included in this version of the V&V documentation. The full set of verification tests for particle tracking will be included in the next version of this document.

Test cases for some other capabilities (such as air/water diffusion and use of unstructured grids) and some constitutive relationships (such as rock compressibility, variable thermal conductivity, and equation-of-state models) still need to be developed.

The validation effort assumes that the data will be collected to perform the validation within the LANL YMP. In particular, there are plans to collect suitable data for this validation exercise within the YMP Reactive Tracer Study Task and Dynamic Transport Task.

4.0 VERIFICATION AND VALIDATION PLAN

The V&V tests outlined in this section will apply in their entirety to any version of the code, no matter what platform is being used. The results from different platforms should be identical to within three significant digits, because the only differences in the versions should be differences in machine precision. Table 1 in Appendix B provides a summary of the FEHM requirements and a listing of which problems test them.

DRAFT 4/97

4.1 Testing of Thermodynamic Functions

4.1.1 Purpose

Density, viscosity, and enthalpy are strong functions of pressure (P) and temperature (T). Because FEHM is an implicit code that uses a Newton-Raphson iteration, derivatives of the thermodynamic functions with respect to P and T are also required. The equations for all water properties listed in Section 4.1.4 will be evaluated over the full range of pressure and temperature for which they were created.

The equation for the saturation line is important for the determination of the phase state of the liquid vapor system. The saturation functions will also be evaluated over the full range of pressure and temperature for which they were created.

4.1.2 Functional description

The test suite consists of a set of simple programs that call the FEHM thermodynamic functions with pressures and temperatures in the prescribed ranges. An agreement between values generated by FEHM and values in the *NBS/NRC Steam Tables* (Harr et al. 1984) with a deviation of less than 2% over the entire range of temperatures and pressures will constitute a verification of the FEHM thermodynamics functions.

4.1.3 Assumptions and limitations

The FEHM thermodynamics functions were created for a specified range of temperatures and pressures. The tests are conducted only within the specified range. Valid ranges for each function are given below under the sections entitled **Required Inputs**.

The thermodynamics functions are being tested independently of the FEHM code so do not test the response of the code when pressures or temperatures are out of range. For further discussion of code behavior in these cases, see the previous chapter and the FEHM document "Summary of Models and Methods" (Zyvoloski et al. 1997a).

4.1.4 Summary of test cases

4.1.4.1 Enthalpy

4.1.4.1.1 Function Tested. This test verifies that the rational polynomial expression implemented in FEHM correctly computes the enthalpy as a function of pressure and temperature.

4.1.4.1.2 Test Scope. This test is a verification test.

4.1.4.1.3 Requirements Tested. Requirement 3.3.1, "Pressure- and temperature-dependent water properties," of Chapter I is verified by this test.

4.1.4.1.4 Required Inputs. The pressures (P) and temperatures (T) at which to calculate enthalpy are required: for liquid enthalpies, the range of $0.001 \le P \le 110.0$ MPa and $15 \le T \le 360\,^{\circ}$C; for vapor enthalpies, the range of $0.001 \le P \le 20.0$ MPa and $15 \le T \le 360\,^{\circ}$C.

4.1.4.1.5 Expected Outputs. Values for enthalpy from the FEHM thermodynamics functions will be output and compared to

values obtained from the *NBS/NRC Steam Tables*. Values within 2% of the *Steam Tables* data will be considered acceptable.

4.1.4.2 Density

4.1.4.2.1 Function Tested. This test verifies that the rational polynomial expression implemented in FEHM correctly computes the density as a function of pressure and temperature.

4.1.4.2.2 Test Scope. This test is a verification test.

4.1.4.2.3 Requirements Tested. Requirement 3.3.1, "Pressure- and temperature-dependent water properties," of Chapter I is verified by this test.

4.1.4.2.4 Required Inputs. The pressures (P) and temperatures (T) at which to calculate density are required: for liquid densities, the range of $0.001 \le P \le 110.0$ MPa and $15 \le T \le 360$ °C; for vapor densities, the range of $0.001 \le P \le 20.0$ MPa and $15 \le T \le 360$ °C.

4.1.4.2.5 Expected Outputs. Values for density from the FEHM thermodynamics functions will be output and compared to values obtained from the *NBS/NRC Steam Tables*. Values within 2% of the *Steam Tables* data will be considered acceptable.

4.1.4.3 Compressibility (derivative of density with respect to pressure)

4.1.4.3.1 Function Tested. This test verifies that the rational polynomial expression implemented in FEHM correctly computes the compressibility (derivative of density with respect to pressure) as a function of pressure and temperature.

4.1.4.3.2 Test Scope. This test is a verification test.

4.1.4.3.3 Requirements Tested. Requirement 3.3.1, "Pressure- and temperature-dependent water properties," of Chapter I is verified by this test.

4.1.4.3.4 Required Inputs. The pressures (P) and temperatures (T) at which to calculate compressibility are required: for liquid compressibilities, the range of $0.001 \le P \le 110.0$ MPa and $15 \le T \le 360$ °C, for vapor compressibilities, the range of $0.001 \le P \le 20.0$ MPa and $15 \le T \le 360$ °C.

4.1.4.3.5 Expected Outputs. Values for compressibility from the FEHM thermodynamics functions will be output and compared to values obtained from the *NBS/NRC Steam Tables*. Compressibility is a commonly used property of the fluid but does not appear directly in the equations that are solved and does not affect the solution. The compressibility is not directly derived from the *Steam Tables* data but is computed from the derivative of the density function. Therefore, values within 10% of the *Steam Tables* data will be considered acceptable.

4.1.4.4 Viscosity

4.1.4.4.1 Function Tested. This test verifies that the rational polynomial expression implemented in FEHM correctly

computes the viscosity as a function of pressure and temperature.

4.1.4.4.2 Test Scope. This test is a verification test.

4.1.4.4.3 Requirements Tested. Requirement 3.3.1, "Pressure- and temperature-dependent water properties," of Chapter I is verified by this test.

4.1.4.4.4 Required Inputs. The pressures (P) and temperatures (T) at which to calculate viscosity are required: for liquid viscosities, the range of $0.001 \le P \le 110.0$ MPa and $15 \le T \le 360$ °C; for vapor viscosities, the range of $0.001 \le P \le 20.0$ MPa and $15 \le T \le 360$ °C.

4.1.4.4.5 Expected Outputs. Values for viscosity from the FEHM thermodynamics functions will be output and compared to values obtained from the *NBS/NRC Steam Tables*. Values within 2% of the *Steam Tables* data will be considered acceptable.

4.1.4.5 Saturation pressure and temperature

4.1.4.5.1 Function Tested. This test verifies that the rational polynomial expression implemented in FEHM correctly computes the pressure as a function of saturation temperature and the temperature as a function of saturation pressure.

4.1.4.5.2 Test Scope. This test is a verification test.

4.1.4.5.3 Requirements Tested. Requirement 3.3.2, "Properties of air and air/water vapor mixtures," of Chapter I is verified by this test.

4.1.4.5.4 Required Inputs. The temperatures (T) at which to calculate saturation pressure and the pressures (P) for which to calculate saturation temperature are required: in the range of $0.00123 \le P \le 14.59410$ MPa and $10 \le T \le 340$ °C.

4.1.4.5.5 Expected Outputs. Values for saturation pressure and temperature from the FEHM thermodynamics functions will be output and compared to values obtained from the *NBS/NRC Steam Tables*. Values within 2% of the *Steam Tables* data will be considered acceptable.

4.2 Test of Heat Conduction

4.2.1 Purpose

Though simple heat-conduction simulations without flow are not used in the modeling studies of Yucca Mountain, heat transfer is an important process in many calculations, including potential repository-heating calculations. Furthermore, it is convenient to use the analytical solutions available for 2-D and 3-D heat conduction in solids. The solutions give an excellent check on the purely geometric aspects of the code as well as the finite-element representation of second-order partial differential equations.

The code will be checked against both 2-D and 3-D analytical solutions with regular grid spacing for triangular, rectangular, prism, brick, tetrahedral, and mixed elements. All solutions will be for linear (constant parameter) problems.

4.2.2 Functional description

The test suite consists of a set of simulations, with heat conduction only, that model the same problem using different finite-element meshes. In addition to demonstrating that the heat-conduction problem has been correctly formulated, the test suite will demonstrate that the various element types have been correctly implemented.

4.2.3 Assumptions and limitations

The analytical solutions for 2-D and 3-D heat conduction are provided by Carslaw and Jaeger (1959). For two-dimensional heat conduction in a rectangle, the analytical solution takes the form:

$$T = T_s + \frac{16(T_0 - T_s)}{\pi^2}\left(\sum_{m=0}^{\infty}\sum_{n=0}^{\infty}\frac{(-1)^{m+n}}{(2m+1)(2n+1)}\cos\frac{(2m+1)\pi x}{2a}\cos\frac{(2n+1)\pi y}{2b}e^{-\alpha_{m,n}t}\right) ,$$

where $\alpha_{m,n} = \frac{\kappa\pi^2}{4}\left[\frac{(2m+1)^2}{a^2} + \frac{(2n+1)^2}{b^2}\right]$ and

the region is taken to be $-a < x < a, -b < y < b$.

Extended to three-dimensional heat conduction in a cube:

$$T = T_s + \frac{64(T_0 - T_s)}{\pi^3}\left(\sum_{l=0}^{\infty}\sum_{m=0}^{\infty}\sum_{n=0}^{\infty}\frac{(-1)^{l+m+n}}{(2l+1)(2m+1))(2n+1)}\cos\frac{(2l+1)\pi x}{2a}\cos\frac{(2m+1)\pi y}{2b}\cos\frac{(2n+1)\pi z}{2c}e^{-\alpha_{l,m,n}t}\right) ,$$

where $\alpha_{l,m,n} = \frac{\kappa\pi^2}{4}\left[\frac{(2l+1)^2}{a^2} + \frac{(2m+1)^2}{b^2} + \frac{(2n+1)^2}{c^2}\right]$ and

the rectangular region is taken to be $-a < x < a, -b < y < b, -c < z < c$.

Heat conduction in a solid 1-meter square/cube with an initial temperature T_0 = 200°C is modeled after a surface temperature T_s = 100°C is imposed at time t = 0. Due to symmetry, only a quarter of the square, or an eighth of the cube (0.5 meters on a side), needs to be modeled (see Fig. 1). Table 22 summarizes the rock properties and problem dimensions used for the heat-conduction problem.

DRAFT 4/97

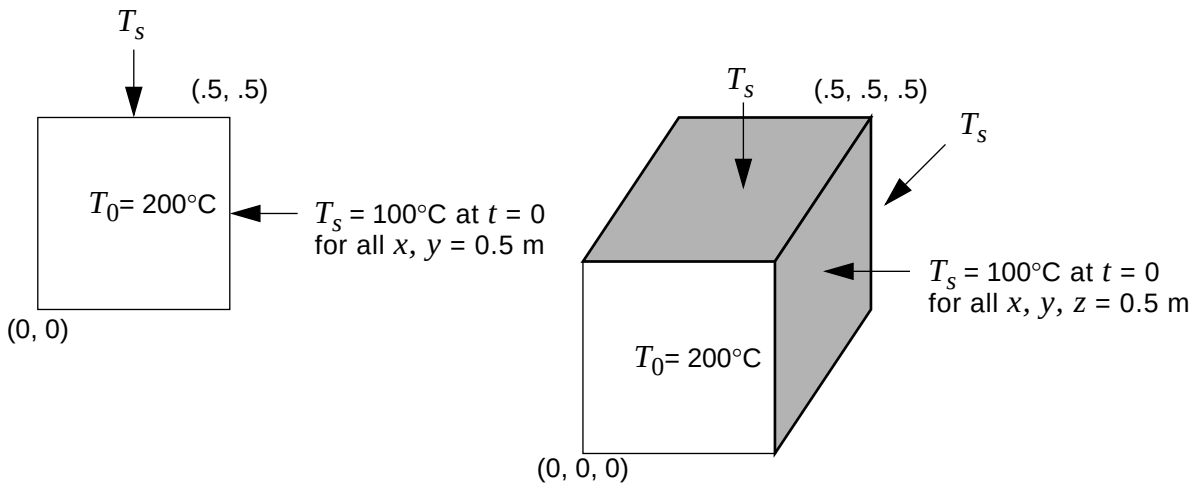

Figure 1. Schematic diagrams of 2-D and 3-D heat-conduction problems.

Table 22. Input parameters for the 2-D and 3-D heat-conduction problems

Parameter	Symbol	Value
Rock thermal conductivity	κ_r	2.7 $\frac{W}{m \cdot K}$
Rock density	ρ_r	2700 kg/m^3
Rock specific heat	C_r	1000 $\frac{J}{kg \cdot K}$
Rock thermal diffusivity	$\kappa = \frac{\kappa_r}{\rho_r C_r}$	10^{-6} m^2/s
Width	a	0.5 m
Length	b	0.5 m
Height	c	0.5 m
Node spacing	Δx, Δy, Δz	0.05 m
Time step	Δt	0.005 days
Total elapsed time	t	4 days (2-D) 3 days (3-D)
Initial temperature	T_0	200°C
Boundary conditions:	At x, y, z = 0.5 m,	$T_s(t)$ = 100°C

DRAFT 4/97

4.2.4 Summary of test cases

4.2.4.1 2-D heat conduction in a square

4.2.4.1.1 Function Tested. This test verifies that FEHM correctly models two-dimensional heat conduction. It also verifies that the 2-D finite-element representation of 3-node triangles (triangular-element meshes), 4-node quadrilaterals (rectangular-element meshes), mixed-element meshes (containing both triangular and rectangular elements), and refined-element meshes (containing rectangular and trapezoidal elements) have been correctly implemented (see Fig. 2).

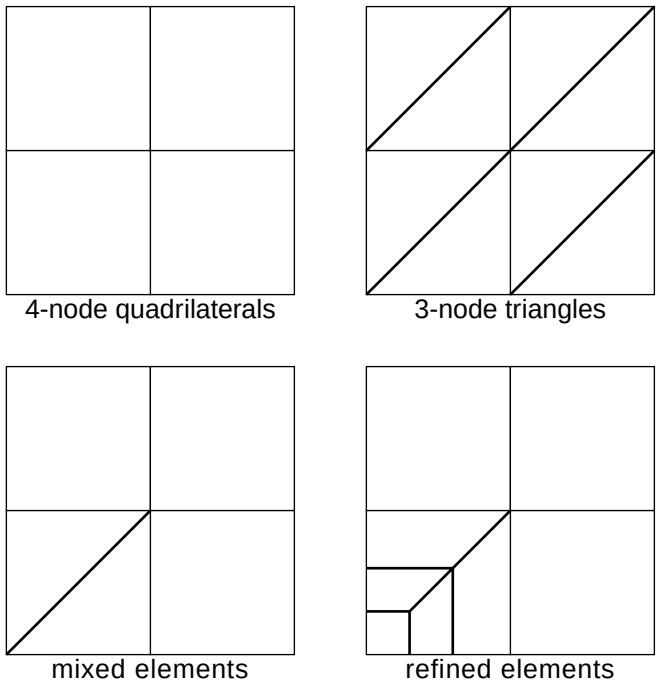

Figure 2. Geometric configurations tested by the 2-D heat-conduction problem.

4.2.4.1.2 Test Scope. This test case is a verification test.

4.2.4.1.3 Requirements Tested. Requirements 3.1, "Finite-element Coefficient Generation," 3.2, "Formulate Transient Equations" (specifically Section 3.2.1), 3.4, "Compute Solution to Transient Equations," and 3.5, "Provide Input/Output Data Files," of Chapter I are verified by this test.

4.2.4.1.4 Required Inputs. Input is provided in the following files:

- *heat2d.in*: basic input data file used in conjunction with the following geometry data files:
- *heat2d.geom.2d_tri*: 3-node triangles (121 nodes, 200 elements),
- *heat2d.geom.2d_quad*: 4-node quadrilaterals (121 nodes, 100 elements),

- *heat2d.geom.2d_mix*: mixed elements, 3-node triangles and 4-node quadrilaterals (121 nodes, 104 elements), or
- *heat2d.geom.2d_ref*: refined elements, 4-node quadrilaterals with refinement about the node at x = y = 0 m (127 nodes, 104 elements).

4.2.4.1.5 Expected Outputs. Values from FEHM for temperature versus time at the center of the square (x = y = 0 m) and values for temperature versus position (x = y) at a specified time (time = 0.25 days) will be output and compared to the analytical solution. Values within 5% of the analytical solution will be considered acceptable.

4.2.4.2 3-D heat conduction in a cube

4.2.4.2.1 Function Tested. This test verifies that FEHM correctly models three-dimensional heat conduction. It also verifies that the finite-element representation of 3-D, 6-node triangular prisms (prism elements), 8-node quadrilateral polyhedrons (brick elements), 4-node tetrahedrals, mixed-element meshes (containing both triangular prisms and quadrilateral polyhedrons), and refined-element meshes (containing quadrilateral polyhedrons and trapezoidal polyhedrons) have been correctly implemented (see Fig. 3). In addition, the finite-volume option, in which the code subdivides brick elements into tetrahedrals, is tested.

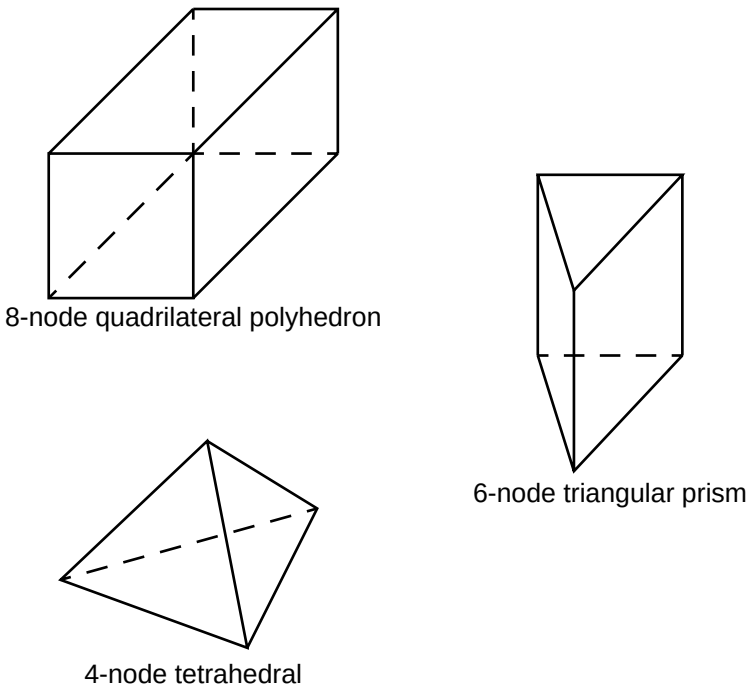

Figure 3. Geometric elements tested by the 3-D heat-conduction problem.

DRAFT 4/97

4.2.4.2.2 Test Scope. This test case is a verification test.

4.2.4.2.3 Requirements Tested. Requirements 3.1, "Finite-element Coefficient Generation," 3.2, "Formulate Transient Equations" (specifically Section 3.2.1), 3.4, "Compute Solution to Transient Equations," and 3.5, "Provide Input/Output Data Files," of Chapter I are verified by this test.

4.2.4.2.4 Required Inputs. Problem input is provided in the following files:

- *heat3d.in*: basic input data file used in conjunction with the following geometry data files:
- *heat3d.geom.3d_tri*: 6-node triangular prisms (1331 nodes, 2000 elements),
- *heat3d.geom.3d_quad*: 8-node quadrilateral polyhedrons (1331 nodes, 1000 elements),
- *heat3d.geom.3d_tets*: 4-node tetrahedrals (1331 nodes, 6000 elements),
- *heat3d.geom.3d_mix*: mixed elements, 6-node triangular prisms and 8-node quadrilateral polyhedrons (1331 nodes, 1020 elements), or
- *heat3d.geom.3d_ref*: refined elements, 8-node quadrilateral polyhedrons with refinement about node at x = y = 0 m for z = 0 to 0.5 m (1364 nodes, 1020 elements); and
- *heat3d.finv.in*: basic input data file using the finite-volume option used in conjunction with the following geometry data files:
- *heat3d.geom.3d_quad* or
- *heat3d.geom.3d_ref*.

4.2.4.2.5 Expected Outputs. Values from FEHM for temperature versus time at the center of the cube (x = y = z = 0 m) and values for temperature versus position (x = y = z) at a specified time (time = 0.25 days) will be output and compared to the analytical solution. Values within 5% of the analytical solution will be considered acceptable.

DRAFT 4/97

4.3 Test of Temperature in a Wellbore

4.3.1 Purpose

The ability to model temperature changes in a wellbore is important to the interpretation of temperature surveys. Ramey (1962) has developed a semianalytical technique for predicting the thermal drawdown in a wellbore. Comparison with this solution will help verify that the code is capable of analyzing temperature logs and, more generally, of handling a thermal-conduction problem coupled to advective heat transport.

4.3.2 Functional description

The test suite consists of a simulation of fluid injection into a wellbore. In addition to demonstrating that the heat- and mass-transfer problem has been correctly formulated, the test suite will demonstrate that the 2-D radial geometry has been correctly implemented.

4.3.3 Assumptions and limitations

Fluid injection at constant temperature, T_{inj}, into a wellbore is modeled (Fig. 4). Flow is confined to the wellbore, i.e., there is no flow between the wellbore and the surrounding rock. The semianalytical solution is given by

$$T_f(z,t) = b + az - aA + (T_{inj} - b + aA)e^{-\frac{z}{A}},$$

where $A = \frac{qcf(t)}{2\pi\kappa}$ and $f(t) = \frac{1}{\frac{4}{\pi^2}\int_0^\infty \frac{e^{-\alpha u^2 t}du}{u(J_0^{\,2}(r_w u) + Y_0^{\,2}(r_w u))}}$.

J_0 and Y_0 are Bessel functions of the first and second kind, of order 0, respectively. The initial temperature distribution in the medium is given by a linear geothermal gradient $T_r = b + az$, where b is the surface rock temperature and a is the geothermal gradient. Although the Ramey solution models a semi-infinite reservoir in the radial direction, for the FEHM model, the reservoir radius has been set to 40 m. Table 23 defines the input parameters used for FEHM and the Ramey analytical solution.

4.3.4 Summary of test cases

4.3.4.1 Constant-temperature injection into a wellbore

4.3.4.1.1 Function Tested. This test verifies that FEHM has correctly implemented the heat- and mass-transfer problem and 2-D radial geometry.

4.3.4.1.2 Test Scope. This test case is a verification test.

4.3.4.1.3 Requirements Tested. Requirements 3.1, “Finite-element Coefficient Generation,” 3.2, “Formulate Transient Equations” (specifically Sections 3.2.2 and 3.2.6), 3.3, “Apply Constitutive Relationships” (specifically Section 3.3.1), 3.4, “Compute Solution to Transient Equations,” and 3.5, “Provide Input/ Output Data Files,” of Chapter I are verified by this test.

DRAFT 4/97

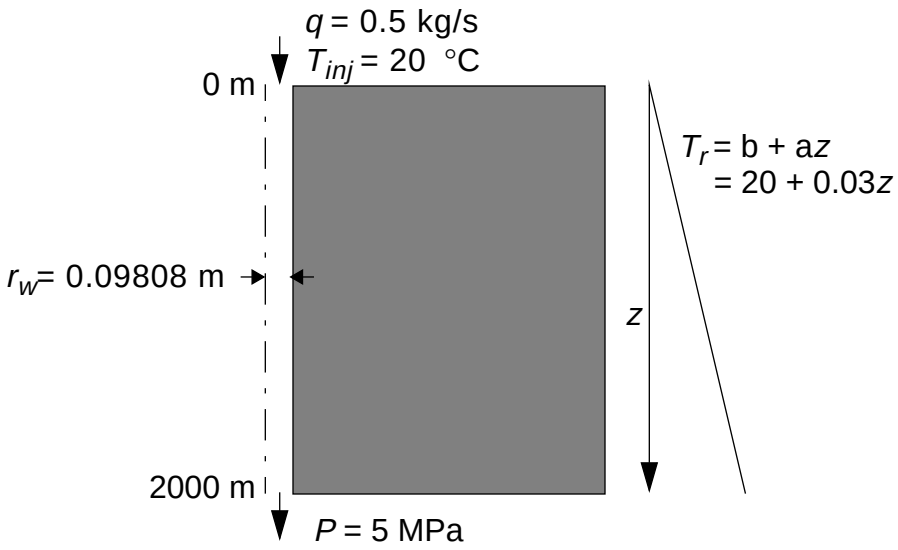

Figure 4. Schematic drawing of the problem geometry and boundary conditions for the temperature-in-a-wellbore problem.

4.3.4.1.4 Required Inputs. Problem input is provided in the following files:

- *ramey.in*: basic input data and
- *ramey.geom*: geometry data (1010 nodes, 900 elements).

4.3.4.1.5 Expected Outputs. Values from FEHM for temperature versus time at fixed depth (d = 1000 and 2000 m) and values for temperature versus depth (d = 0 to 2000 m) at a specified time (t = 25 days) will be output and compared to the analytical solution. Values within 5% of the analytical solution will be considered acceptable.

DRAFT 4/97

Table 23. Input parameters for the temperature-in-a-wellbore problem

Parameter	Symbol	Value
Rock thermal conductivity	κ_r	2.7 $\frac{W}{m \cdot K}$
Rock density	ρ_r	2700 kg/m^3
Rock specific heat	C_r	1000 $\frac{J}{kg \cdot K}$
Rock thermal diffusivity	$\alpha_r = \frac{\kappa_r}{\rho_r C_r}$	10^{-6} m^2/s
Rock (matrix) permeability	k	10^{-20} m^2
Porosity	f	0
Fluid heat capacity	C_f	4200 $\frac{J}{kg \cdot K}$
Wellbore radius	r_w	0.09808 m
Radial extent	r	40 m
Node spacing (radial)	Δr	0.19616 - 17.25495 m
Well depth	z	2000 m
Node spacing (vertical)	Δz	20 m
Surface rock temperature	b	20°C
Geothermal gradient	a	0.03°C/m
Injection rate	q	0.5 kg/s
Injection temperature	T_{inj}	20°C
Time step	Δt	0.001 - 1 days
Total elapsed time	t	25 days
Initial temperature distribution (T in °C, z in m): $T(z) = 20 + 0.03\ z$ for r = 0 - 40 m		
Boundary conditions: At r = 0 m, z = 0 m, q = 0.5 kg/s, T_{inj} = 20°C; At r = 0 m, z = 2000 m, $P(t)$ = 5 MPa		

DRAFT 4/97

4.4 Test of Pressure Transient Analysis

4.4.1 Purpose

Properties of underground reservoirs are often determined by pressure tests. Theis (1935) developed a solution for radial flow to a well in the form of pressure as a function of time and the spatial coordinates. Comparison with this solution will help demonstrate that the pressure equation (the conservation of mass with Darcy's law) is implemented correctly.

4.4.2 Functional description

The test suite consists of a simulation of 1-D radial flow into an infinite aquifer. In addition to demonstrating that the transient pressure equation has been correctly formulated, the test suite will demonstrate that the radial geometry has been correctly implemented.

4.4.3 Assumptions and limitations

Injection into a centrally located well at a constant volumetric rate, q, is modeled. The well (modeled as a line source) is assumed to be situated in a porous medium of infinite radial extent. The analytical solution (from Matthews and Russell 1967) is given by

$$p(r,t) = p_i - \frac{q\mu}{2\pi kh}\left[-\frac{1}{2}E_i\left(-\frac{\phi\mu c r^2}{4kt}\right)\right] ,$$

where the exponential integral function is $-E_i(-x) = \int_x^\infty \frac{e^{-u}}{u}du$.

Figure 5 shows the problem geometry and boundary conditions. This problem is isothermal. Input parameters defining the problem are given in Table 24.

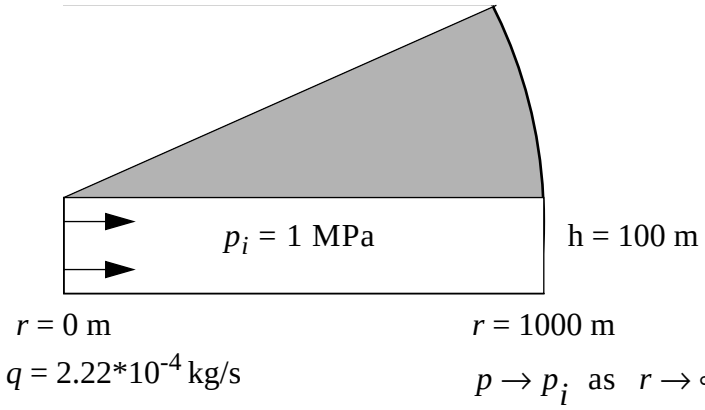

Figure 5. Schematic drawing of the problem geometry and boundary conditions for the transient pressure problem.

Table 24. Input parameters for the transient pressure problem

Parameter	Symbol	Value
Reservoir permeability in radial direction	k	10^{-14} m^2
Reservoir porosity	ϕ	0.4
Fluid compressibility	c	$5.06*10^{-4}$ MPa^{-1}
Fluid viscosity	μ	$5.48*10^{-4}$ Pa•s
Reservoir thickness	h	100 m
Node spacing (vertical)	Δh	100 m
Reservoir length (radial)	r	0 - 1000 m
Node spacing (radial)	Δr	0.00144 - 107 m
Flow rate	q	$2.22*10^{-4}$ kg/s
Initial pressure	p_i	1 MPa
Temperature (isothermal)	T	50°C
Time step	Δt	300 s
Total elapsed time	t	1 day

Boundary conditions: $p \rightarrow p_i$ as $r \rightarrow \infty$

$$\lim_{r \to 0} r\frac{\partial p}{\partial r} = \frac{q\mu}{2\pi kh}$$ (constant flow at r = 0, line source)

4.4.4 Summary of test cases

4.4.4.1 Radial flow from a well

4.4.4.1.1 Function Tested. This test verifies that FEHM has correctly implemented the pressure equations, i.e., the conservation of mass with Darcy's law.

4.4.4.1.2 Test Scope. This test case is a verification test.

4.4.4.1.3 Requirements Tested. Requirements 3.1, "Finite-element Coefficient Generation," 3.2, "Formulate Transient Equations" (specifically Sections 3.2.2 and 3.2.6), 3.4, "Compute Solution to Transient Equations," and 3.5, "Provide Input/Output Data Files," of Chapter I are verified by this test.

DRAFT 4/97

4.4.4.1.4 Required Inputs. Problem input is provided in the following file:

- *theis.in*: basic input and geometry data (202 nodes, 100 elements).

4.4.4.1.5 Expected Outputs. Values from FEHM, for pressure versus time, at fixed radii (r = 0.00144 and 3.44825 m), and values for pressure versus radius (r = 0 to 1000 m), at a specified time (t = 1 day), will be output and compared to the analytical solution. Values within 5% of the analytical solution will be considered acceptable.

DRAFT 4/97

4.5 Test of Infiltration into a One-dimensional, Layered, Unsaturated Medium

4.5.1 Purpose

Modeling infiltration into an unsaturated medium can be performed by implementing either the equivalent-continuum method (ECM) or the double-porosity/double-permeability method (DKM). The ECM provides a lumped set of properties for the material that are derived from the separate matrix and fracture properties along with hydrologic conditions such as saturation and pressure. The DKM considers the fractures as a continuous medium and the matrix as another continuous medium and provides for conductance between the two. See the FEHM document "Summary of Methods and Models" (Zyvoloski et al. 1997a, Section 8.2) for more details of the double-porosity/double-permeability method. The DKM requires twice as many finite-element nodes and hence takes longer to run than the ECM. Both methods use the same set of van Genuchten capillary-pressure model parameters to describe the hydrologic properties. The two methods are often compared with each other to assess whether the additional computational burden associated with the DKM is necessary to capture behavior such as fast flow paths in fractures, which are smoothed out in the composite-property model of the ECM. This set of tests verifies that each method, the ECM and the DKM, are implemented properly.

4.5.2 Functional description

The test problem, described by Ho (1995a, 1995b), consists of simulations of infiltration into a one-dimensional column. The column is a transect through a system of four stratigraphic units, each characterized by a unique set of parameters describing the matrix and fracture properties. The stratigraphic system is a representation of the lithologic layering at Yucca Mountain. The four units are the Tiva Canyon welded tuff (TCw), the Paintbrush nonwelded tuff (PTn), the Topopah Springs welded tuff (TSw), and the Calico Hills nonwelded vitrophere (CHnv). A schematic of the thicknesses and layering of the four units considered is shown in Fig. 6. The properties for these four units were taken from YMP total system performance assessment of 1993 (Wilson 1994) and are located in the required inputs files. Key aspects of this data set include matrix intrinsic permeabilities and matrix residual saturations, each of which span four orders of magnitude over the various units.

The test will demonstrate that the equivalent-continuum method and the double-porosity/double-permeability method have been correctly implemented through comparison with simulations performed with TOUGH2, another well-documented model capable of solving this problem (Pruess 1991).

4.5.3 Assumptions and limitations

Infiltration of 4 mm/yr is applied at the top of the system. For the DKM simulations, it is applied to the fracture nodes only. The bottom boundary for all tests is assumed to be the water table, so full saturation is set there. The TOUGH2 simulations with which FEHM will be compared were run at Sandia National Laboratories using TOUGH2 - version 1.1 (April 1993). This is an isothermal air-water problem. Input parameters defining the problem are given in Table 25.

DRAFT 4/97

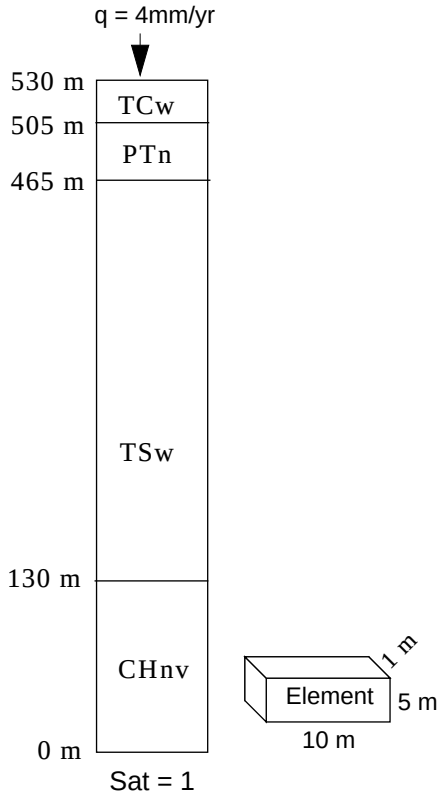

Figure 6. Schematic drawing of the problem geometry for the test of the one-dimensional infiltration problem.

Table 25. Input parameters for the one-dimensional infiltration problem

Parameter	Symbol	Value
Fracture permeability		
TCw	k_f	$2.04*10^{-18}$ m^2
PTn		$2.51*10^{-14}$ m^2
TSw		$2.09*10^{-18}$ m^2
CHnv		$1.10*10^{-16}$ m^2
Matrix permeability		
TCw	k_m	$4.06*10^{-9}$ m^2
PTn		$7.14*10^{-9}$ m^2
TSw		$4.57*10^{-9}$ m^2
CHnv		$6.53*10^{-9}$ m^2

DRAFT 4/97

Table 25. Input parameters for the one-dimensional infiltration problem (continued)

Parameter	Symbol	Value
Fracture porosity (volume fraction for fracture node)		
TCw	$\phi_f\ (V_f)$	$2.93*10^{-4}$
PTn		$9.27*10^{-5}$
TSw		$2.43*10^{-4}$
CHnv		$1.11*10^{-4}$
Matrix porosity		
TCw	ϕ_m	0.087
PTn		0.421
TSw		0.139
CHnv		0.331
Matrix-node length scale		
TCw	L_{f1}	0.18 m
PTn		0.64 m
TSw		0.21 m
CHnv		0.46 m
Column width	w	10 m
Node spacing (horizontal)	Δw	10 m
Column height (elevation)	h	0 - 530 m
Node spacing (vertical)‡	Δh	5 m
Reference pressure	P_r	0.1 MPa
Reference temperature	T_r	20°C
Maximum saturation	S_{lmax}	1.0
Fracture residual saturation	$S_{lr,f}$	0.03
Matrix residual saturation		
TCw	$S_{lr,m}$	0.0212
PTn		0.154
TSw		0.0453
CHnv		0.0968
van Genuchten model parameters for the fracture		
Inverse of air entry pressure		
TCw	$\alpha_{G,f}$	$12.05\ m^{-1}$
PTn		$2.5\ m^{-1}$
TSw		$11.96\ m^{-1}$
CHnv		$2.5\ m^{-1}$

Table 25. Input parameters for the one-dimensional infiltration problem (continued)

Parameter	Symbol	Value
Power in formula		
TCw	n_f	3.0
PTn		3.0
TSw		3.0
CHnv		3.0
van Genuchten model parameters for the matrix		
Inverse of air entry pressure		
TCw	$\alpha_{G,m}$	0.00715 m^{-1}
PTn		0.371 m^{-1}
TSw		0.0133 m^{-1}
CHnv		0.0273 m^{-1}
Power in formula		
TCw	n_m	1.62
PTn		2.37
TSw		1.8
CHnv		2.46
Initial fracture saturation	$S_{l0,f}$	0.5
Initial matrix saturation		
TCw	$S_{l0,m}$	0.95
PTn		0.31
TSw		0.95
CHnv		0.85
Time step	Δt	1 - 1*10^{-8} days
Total elapsed time	t	1*10^{-9} days
Boundary conditions: At h = 530 m	q = 4 mm/yr	
At h = 0 m	S = 1.0	

‡ For the FEHM simulation, an additional node was added at each material interface to facillitate comparison with TOUGH2, which uses cell-centered elements, whereas FEHM uses node-centered elements.

4.5.4 Summary of test cases

4.5.4.1 Test of infiltration into a one-dimensional, layered, unsaturated medium using the equivalent-continuum method (ECM)

4.5.4.1.1 Function Tested. This test verifies that FEHM has correctly implemented for simulations of infiltration into a one-dimensional, layered, unsaturated medium using ECM.

4.5.4.1.2 Test Scope. This test case is a verification test.

4.5.4.1.3 Requirements Tested. Requirements 3.1, “Finite-element Coefficient Generation,” 3.2, “Formulate Transient Equations”

(specifically Sections 3.2.2 and 3.2.6), 3.3, "Apply Constitutive Relationships" (specifically Section 3.3.4), 3.4, "Compute Solution to Transient Equations," and 3.5, "Provide Input/ Output Data Files," of Chapter I are verified by this test.

4.5.4.1.4 Required Inputs. Problem input is provided in the following files:

- *infiltration.ecm.in*: basic input data, case 1, and
- *infiltration.geom*: geometry data used for the above cases.

4.5.4.1.5 Expected Outputs. Values from FEHM for saturation versus elevation will be output, nondimensionalized, and compared to the TOUGH2 solution. A root-mean-square error of the difference between the two simulations less than or equal to 0.05 will be considered acceptable.

4.5.4.2 Test of infiltration into a one-dimensional, layered, unsaturated medium using the double-porosity/double-permeability method (DKM)

4.5.4.2.1 Function Tested. This test verifies that FEHM has been correctly implemented for simulations of infiltration into a one-dimensional, layered, unsaturated medium using DKM.

4.5.4.2.2 Test Scope. This test case is a verification test.

4.5.4.2.3 Requirements Tested. Requirements 3.1, "Finite-element Coefficient Generation," 3.2, "Formulate Transient Equations" (specifically Sections 3.2.2 and 3.2.6), 3.3, "Apply Constitutive Relationships" (specifically Sections 3.3.4 and 3.3.8), 3.4, "Compute Solution to Transient Equations," and 3.5, "Provide Input/Output Data Files," of Chapter I are verified by this test.

4.5.4.2.4 Required Inputs. Problem input is provided in the following files:

- *infiltration.dpm.in*: basic input data, case 2, and
- *infiltration.geom*: geometry data used for the above cases.

4.5.4.2.5 Expected Outputs. Values from FEHM for saturation versus elevation will be output, nondimensionalized, and compared to the TOUGH2 solution. A root-mean-square error of the difference between the two simulations less than or equal to 0.05 will be considered acceptable.

DRAFT 4/97

4.6 Test of Vapor Extraction from an Unsaturated Reservoir

4.6.1 Purpose

The ability to model vapor/gas transport in unsaturated media is important to the design of vapor-extraction sytems and interpretation of their performance. Analytical solutions of steady-state gas flow to a soil vapor-extraction well in the unsaturated zone have been described by Shan et al. (1992). Comparison with this solution will help verify that vapor/gas transport has been correctly implemented in FEHM.

4.6.2 Functional description

The test suite consists of two simulations of steady, 2-D radial soil-vapor flow to a well in an unsaturated reservoir. The first case uses an isotropic permeability model, whereas the second case models an anisotropic reservoir. In addition to demonstrating that the gas-flow problem has been correctly formulated for isotropic and anisotropic permeability models, the test suite will demonstrate that the 2-D radial coordinate geometry has been correctly implemented.

4.6.3 Assumptions and limitations

The analytical solution for pressure for this test case is expressed as an infinite series:

$$P = \frac{\bar{q}}{4\pi\alpha_r}\left[\ln\left(\frac{a-z+[\hat{r}^2+(a-z)^2]^{-1/2}}{b-z+[\hat{r}^2+(b-z)^2]^{-1/2}}\cdot\frac{b+z+[\hat{r}^2+(b+z)^2]^{-1/2}}{a+z+[\hat{r}^2+(a+z)^2]^{-1/2}}\right)-\right.$$

$$\sum_{n=1}^{\infty}(-1)^n\ln\left(\frac{a+z+2nh+[\hat{r}^2+(a+z+2nh)^2]^{-1/2}}{b+z+2nh+[\hat{r}^2+(b+z+2nh)^2]^{-1/2}}\cdot\right.$$

$$\frac{a+z-2nh+[\hat{r}^2+(a+z-2nh)^2]^{-1/2}}{b+z-2nh+[\hat{r}^2+(b+z-2nh)^2]^{-1/2}}\cdot$$

$$\frac{-a+z+2nh+[\hat{r}^2+(-a+z+2nh)^2]^{-1/2}}{-b+z+2nh+[\hat{r}^2+(-b+z+2nh)^2]^{-1/2}}\cdot$$

$$\left.\left.\frac{-a+z-2nh+[\hat{r}^2+(-a+z-2nh)^2]^{-1/2}}{-b+z-2nh+[\hat{r}^2+(-b+z-2nh)^2]^{-1/2}}\right)\right],$$

where $\bar{q} = \dfrac{2P_a q_m}{(a-b)\phi\rho_g}$, $\alpha_r = \dfrac{k_r P_a}{\phi\mu_g}$, $\hat{r} = \left(\dfrac{k_z}{k_r}\right)^{1/2} r$,

r is the radial distance, z is the vertical distance, h is the depth to the water table (impermeable boundary), and a and b are the depths to the bottom and top of the open wellbore interval, respectively. A sensitivity study of

the number of terms required for the solution to achieve a precision of 10^{-3} Pa shows that no more than 50 terms are needed.

The geometry and boundary conditions are shown in Fig. 7. The upper surface is at atmospheric pressure and the remaining edges are impermeable; there are no flow boundaries, with the exception of the extraction wellbore. The problem is isothermal. Values of the analytical solution are inaccurate in the region surrounding the extraction wellbore ($r \leq 0.05$ m, $2.8 \leq z \leq 7.2$ m), so they are excluded from the results used for comparison. Table 26 lists the input parameters for the vapor-extraction problem. The solution is verified by comparison of FEHM results to the analytical solution.

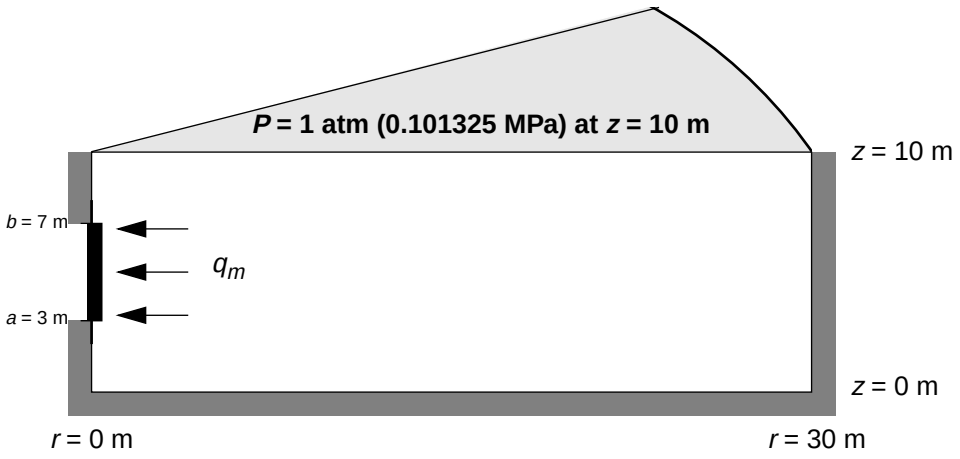

Figure 7. Schematic diagram of the geometry and boundary conditions for the vapor-extraction problem.

Table 26. Input parameters for the vapor-extraction problem

Parameter	Symbol	Value
Reservoir permeability		
Isotropic case	k_r , k_z	10^{-11} m^2
Anisotropic case -radial	k_r	10^{-11} m^2
Anisotropic case -vertical	k_z	10^{-12} m^2
Reservoir porosity	ϕ	0.4
Reservoir length	r	0 - 30 m
Node spacing (radial)	Δr	0.0001 - 1 m
Reservoir thickness (elevation)	h	0 - 10 m
Node spacing (vertical)	Δh	0.5 m

Table 26. Input parameters for the vapor-extraction problem (continued)

Extraction interval, bottom	a	3 m
Extraction interval, top	b	7 m
Ambient (reference) temperature	T_a	10°C
Ambient pressure	P_a	0.101325 MPa
Initial pressure	P_0	0.101325 MPa
Initial saturation	S_0	0.05
Residual liquid saturation	S_{lr}	0.10
Maximum liquid saturation	S_{lmax}	0.99
van Genuchten model parameters		
Inverse of air entry pressure	α_G	0.005 m^{-1}
Power in formula	n	1.8
Gas density	ρ_g	1.24 kg/m^3
Gas viscosity	μ_g	1.76 x 10^{-5} Pa•s
Extraction rate		
Isotropic case	q_m	0.0825 kg/s
Anisotropic case		0.05 kg/s
Time step	Δt	0.001 - 75 days
Total elapsed time		
Isotropic case	t	365 days
Anisotropic case		730 days
Boundary conditions:	At z = 10 m	P = 0.101325 MPa, S = 0.05
	At r = 0 m, 3 ≤ z ≤ 7 m	$q = q_m$
	(Line sink wellbore, z positive upwards)	

4.6.4 Summary of test cases

4.6.4.1 Vapor extraction from an unsaturated reservoir

4.6.4.1.1 Function Tested. This test verifies that FEHM has correctly implemented the gas-flow option of the code for radial flow.

4.6.4.1.2 Test Scope. This test case is a verification test.

4.6.4.1.3 Requirements Tested. Requirements 3.1, "Finite-element Coefficient Generation," 3.2, "Formulate Transient Equations" (specifically Sections 3.2.3 and 3.2.6), 3.3, "Apply Constitutive Relationships" (specifically Sections 3.3.2 and 3.3.4), 3.4, "Compute Solution to Transient Equations," and 3.5, "Provide Input/Output Data Files," of Chapter I are verified by this test.

4.6.4.1.4 Required Inputs. Problem input is provided in the following files:

- *vapextract_iso.in*: basic input data, isotropic case,
- *vapextract_aniso.in*: basic input data, anisotropic case, and
- *vapextract.geom*: geometry data used for the above cases.

4.6.4.1.5 Expected Outputs. Values from FEHM for the steady-state vapor pressure at each node (reached after 365 days for the isotropic case, 730 days for the anisotropic case) will be output and compared to the analytical solution from Shan et al. (1992). Values within 5% of the analytical solution or a root-mean-square error of the difference between the two simulations less than or equal to 0.01 will be considered acceptable.

4.7 Test of Dual Porosity

4.7.1 Purpose

The dual-porosity formulation is a computationally efficient way to model flow in a porous media with high-permeability fractures embedded in low-permeability matrix material. It has previously been shown by Moench (1984) that dual-porosity flow can explain some of the well test data at Yucca Mountain. Warren and Root (1963) provide an analytical solution for dual-porosity flow to a wellbore. This test will check the pressure solution for the dual-porosity coding in FEHM.

4.7.2 Functional description

The test suite consists of a set of simulations of dual-porosity flow to a wellbore. It will demonstrate that the dual-porosity formulation has been correctly implemented.

4.7.3 Assumptions and limitations

Warren and Root have defined the dimensionless pressure drop as

$$\psi_f(1,\tau) \approx \frac{1}{2}\left\{ \ln\tau + 0.80908 + Ei\left[\frac{-\lambda\tau}{\omega(1-\omega)}\right] - Ei\left[\frac{-\lambda\tau}{1-\omega}\right]\right\} \quad ,$$

where $\tau = \dfrac{\overline{k_f}\, t}{\phi_m c_m + \phi_f c_f}$,

$\overline{k_f} = \sqrt{k_{fx} k_{fy}}$,

$\lambda = \dfrac{\alpha k_m r_w^{\,2}}{\overline{k_f}}$,

$\omega = \dfrac{\phi_f c_f}{\phi_m c_m + \phi_f c_f}$,

and Ei is the exponential integral function (see Section 4.3.3). In this solution, τ is dimensionless time, $\overline{k_f}$ is the effective permeability of the anisotropic medium, λ is a measure of the size of the matrix region, ω represents the strength of coupling between the fracture and the matrix, and α is a characteristic dimension.

Figure 8 illustrates the problem geometry and boundary conditions. The input parameters are defined in Table 27. The analytical solution uses a steady-state approximation for the matrix flow (only one matrix node exists per fracture node), so no transient effects are possible in the matrix. The FEHM dual-porosity implementation uses a transient approximation for the matrix material (two matrix nodes exist for each fracture node), so crude transient responses are possible because of flow between two matrix nodes. See the FEHM document “Methods and Models” (Zyvoloski et al. 1997a, Section 8.2) for more details and a description of the model parameters (L_f and V_f). The steady-state approximation is known to be inaccurate at small times (see Warren and Root 1963, p. 248) and is only valid for τ greater than ~100.

DRAFT 4/97

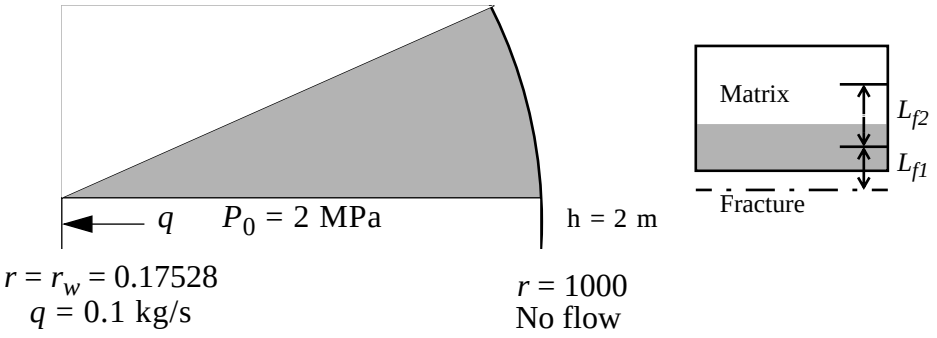

Figure 8. Schematic diagram of the geometry and boundary conditions for the dual-porosity problem.

Table 27. Input parameters for the dual-porosity problem

Parameter	Symbol	Value
Permeability		
fracture	k_f	0.4 x 10^{-12} m^2
matrix (1)		1.904 x 10^{-16} m^2
matrix (2)		1.904 x 10^{-13} m^2
matrix (3)		1.194 x 10^{-14} m^2
Porosity		
fracture	ϕ_f	1.0
matrix (1)		0.06081
matrix (2)		0.6081
matrix (3)		0.47
Volume fraction		
fracture node (1)(2)	V_f	0.006711409
fracture node (3)		0.000476417
first matrix node (1)(2)	V_{f1}	0.335570470
first matrix node (3)		0.333492139
Length scale (1)(2)	L_{f0}	0.10
Length scale (3)		0.01
Compressibility (fracture and matrix)	c_f, c_m	5.503e-4 MPa^{-1}

Number in ( ) denotes for which case that value was used.

Table 27. Input parameters for the dual-porosity problem (continued)

Parameter	Symbol	Value
Flow rate	q	0.1 kg/s
Viscosity	μ	1.0021e-3 Pa•s
Reference temperature	T	20°C
Initial pressure	P_0	2.0 MPa
Wellbore radius	r_w	0.17528 m
Reservoir length	r	0 - 1000 m
Node spacing (radial) [average of graded mesh 1.0 m]	Δr	0.07 - 10 m
Reservoir height	h	2 m
Node spacing (vertical)	Δh	2 m
Time step (1)	Δt	$1.0*10^{-8}$ - 0.01 days
Time step (2)(3)	Δt	$2.0*10^{-7}$ - 0.01 days
Total elapsed time (1)	t	0.1 days
Total elapsed time (2)(3)	t	0.2 days
Boundary conditions:	At r = r_w = 0.17528 m	q = 0.1 kg/s
	At r = 1000 m	No flow boundary
	(Sufficiently large to approximate semi-infinite reservoir)	
Number in ( ) denotes for which case that value was used.		

4.7.4 Summary of test cases

4.7.4.1 Dual-porosity problem

4.7.4.1.1 Function Tested. This test verifies that FEHM has correctly implemented the dual-porosity formulation.

4.7.4.1.2 Test Scope. This test case is a verification test.

4.7.4.1.3 Requirements Tested. Requirements 3.1, “Finite-element Coefficient Generation,” 3.2, “Formulate Transient Equations” (specifically Sections 3.2.2 and 3.2.6), 3.3, “Apply Constitutive Relationships” (specifically Sections 3.3.1 and 3.3.7), 3.4, “Compute Solution to Transient Equations,” and 3.5, “Provide Input/Output Data Files,” of Chapter I are verified by this test.

4.7.4.1.4 Required Inputs. Problem input is provided in the following files:

- *dual1.in*: basic input data, case 1,
- *dual2.in*: basic input data, case 2,
- *dual3.in*: basic input data, case 3, and
- *dual.geom*: geometry data used for the above cases.

4.7.4.1.5 Expected Outputs. Values from FEHM for pressure versus time at the wellbore fracture node, $r = 0.1398$ (i.e., interior node closest to $r_w = 0.17528$), will be output, nondimensionalized, and compared to the Warren and Root analytical solution. Values within 5% of the analytical solution for $\tau > 100$ will be considered acceptable.

DRAFT 4/97

4.8 Test of Heat and Mass Transfer in Porous Media

4.8.1 Purpose

In some special instances, the flow of a hot fluid in a confined aquifer may be described by an analytical expression. Avdonin (1964) presents an analytical solution for one-dimensional, radial fluid flow with heat conduction in the orthogonal direction. In addition to testing the coupled heat- and mass-transfer implementation for a single-phase system, the results will also demonstrate that the radial geometry is correctly implemented with different grid spacings.

4.8.2 Functional description

The test suite consists of a set of simulations of 1-D radial flow into a confined aquifer. The same flow problem is run with the domain divided into 84 nodes (41 elements), 400 nodes (199 elements), and 800 nodes (399 elements). In addition to demonstrating that the heat- and mass-transfer problem has been correctly formulated and that the radial geometry has been correctly implemented, this test will assess the impact of finer spatial discretization on accuracy.

4.8.3 Assumptions and limitations

The analytical solution presented by Avdonin (1964) takes the form:

$$u(\omega, \tau) = \frac{1}{\Gamma(\nu)}\left(\frac{\omega^2}{4\tau}\right)^{\nu} \int_0^1 \exp\left(-\frac{\omega^2}{4\tau s}\right) erfc\left(\frac{\alpha s\sqrt{\tau}}{2\sqrt{1-s}}\right)\frac{ds}{s^{\nu+1}} \quad ,$$

where $\omega = \frac{2r}{b}$,

$$\tau = \frac{4\kappa_t t}{c_t \rho_t b^2} \ ,$$

$$\nu = \frac{q c_w \rho_w}{4\pi b \kappa_t} \ ,$$

$$\alpha = \left(\frac{\kappa_r c_r \rho_r}{\kappa_t c_t \rho_t}\right)^{1/2} \quad ,$$

erfc is the complimentary error function, Γ is the gamma function, r is the radial coordinate, q is the injection flow rate, u is a dimensionless temperature change, and the integration variable s represents a dimensionless time. The subscripts r, w, and t refer to rock, water, and total (rock and water), respectively. The temperature is computed using:

$$T = T_0 - u(\omega, \tau) \cdot (T_0 - T_{in}) \ .$$

This problem assumes one-dimensional, radial, steady-state flow and unsteady heat transport in a single-phase liquid. It simulates the injection of cool water into a geothermal reservoir. Figure 9 shows the problem geometry with boundary and initial conditions. Input parameters defining the problem are given in Table 28.

DRAFT 4/97

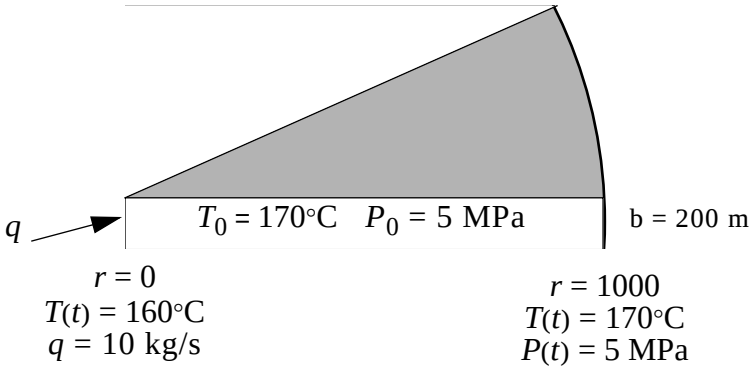

Figure 9. Schematic diagram of the Avdonin problem geometry with boundary and initial conditions.

4.8.4 Summary of test cases

4.8.4.1 Heat and mass transfer in a 1-D radial aquifer

4.8.4.1.1 Function Tested. This test verifies that FEHM correctly models 1-dimensional heat and mass transport for radial flow and demonstrates the impact of finer spatial discretization on accuracy.

4.8.4.1.2 Test Scope. This test case is a verification test.

4.8.4.1.3 Requirements Tested. Requirements 3.1, "Finite-element Coefficient Generation," 3.2, "Formulate Transient Equations" (specifically Sections 3.2.2 and 3.2.6), 3.3, "Apply Constitutive Relationships" (specifically Section 3.3.1), 3.4, "Compute Solution to Transient Equations," and 3.5, "Provide Input/ Output Data Files," of Chapter I are verified by this test.

4.8.4.1.4 Required Inputs. Problem input is provided in the following files:

- *avdonin.in*: basic input data used in conjunction with the following geometry data files:
- *avdonin.geom.84*: (84 nodes, 42 elements),
- *avdonin.geom.400:* (400 nodes, 199 elements), or
- *avdonin.geom.800:* (800 nodes, 399 elements).

4.8.4.1.5 Expected Outputs. Values from FEHM, for temperature versus time at a fixed radius (r = 37.5 m), and values for temperature versus radius (r = 0 to 1000 m) at a specified time, (t = 1.e9 s) will be output and compared to the analytical solution. Values within 5% of the analytical solution will be considered acceptable.

DRAFT 4/97

Table 28. Input parameters for the Avdonin problem

Parameter	Symbol	Value
Reservoir permeability	k	10^{-12} m^2
Reservoir porosity	ϕ	0.2
Rock thermal conductivity	k_r	20 $\frac{W}{m \cdot K}$
Rock density	ρ_r	2500 kg/m^3
Rock specific heat	C_r	1000 $\frac{J}{kg \cdot K}$
Reservoir thickness	b	200 m
Node spacing (vertical)	Δb	200 m
Reservoir length (radial)	r	0 - 1000 m
Node spacing (radial) 84-node domain 400-node domain 800-node domain	Δr	 25 m 0.64 - 12 m 0.32 - 12 m
Injection rate	q	10 kg/s
Injection temperature	T_{in}	160°C
Initial temperature	T_0	170°C
Initial pressure	P_0	5 MPa
Time step	Δt	50 days
Total elapsed time	t	1*10^9 s
Boundary conditions:	At $r = r_w = 0$ m,	$T(t) = 160$°C, $q = 10$ kg/s
	At $r = 1000$ m,	$T(t) = 170$°C, $P(t) = 5$ MPa

DRAFT 4/97

4.9 Test of Toronyi Two-phase Problem

4.9.1 Purpose

This problem has evolved into a standard test case for checking two-phase heat and mass transfer (Toronyi and Farouq Ali 1977). Fluid is discharged from a two-phase geothermal reservoir, and the saturation at each node is simulated. There is no analytical solution for this problem; comparisons must be made with other transient heat- and mass-transfer codes. The problem tests the multiphase capabilities severely, and in doing so, verifies that the liquid- and vapor-phase-transport submodels of FEHM are working properly.

4.9.2 Functional description

The test suite consists of a simulation of fluid discharge from a two-phase aquifer. In addition to demonstrating that the heat- and mass-transfer problem has been correctly formulated, it will demonstrate that phase partitioning has been correctly implemented.

4.9.3 Assumptions and limitations

Fluid is discharged at a constant rate from the two-phase geothermal reservoir until 19% of the original water mass has been removed (78.31 days). There is no flow across the peripheral boundaries. Temperature is controlled by the saturation pressure/temperature curve.

The solution is verified by comparison of FEHM results to those found by Thomas and Pierson (1978). Thomas and Pierson used cell-centered elements, wheras FEHM uses node-centered elements, so boundary elements were adjusted to provide matching central nodes. The reservoir model (solution domain) is shown in Fig. 10 along with the node saturations obtained by Thomas and Pierson. The asymmetry in the solution is due to the off-center location of the discharge node. Table 29 lists the input parameters for the Toronyi problem.

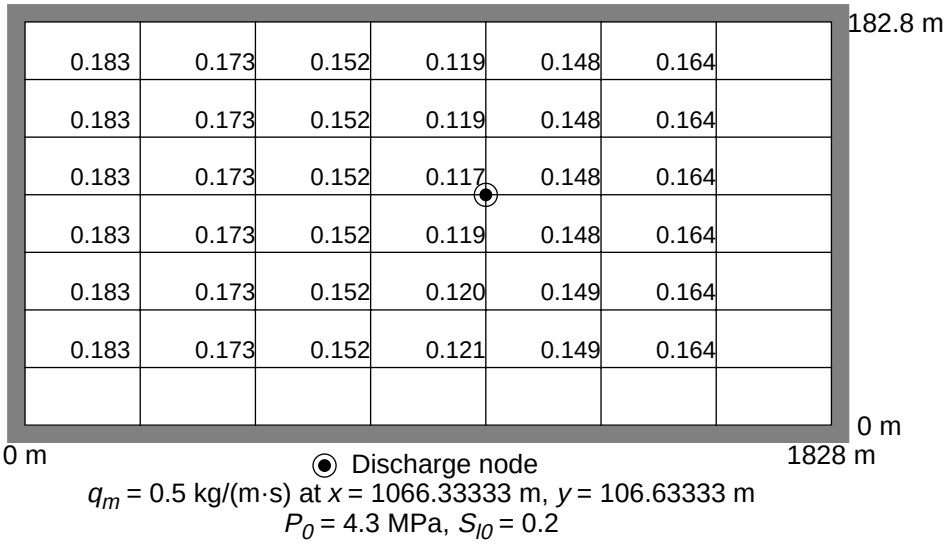

Figure 10. Solution domain and saturation results for the Toronyi problem.

DRAFT 4/97

Table 29. Input parameters for the Toronyi two-phase problem

Parameter	Symbol	Value
Reservoir permeability	k	9.869 x 10^{-13} m^2
Reservoir porosity	ϕ	0.05
Rock thermal conductivity	κ_r	1.73 $\frac{W}{m \cdot K}$
Rock density	ρ_r	2500 kg/m^3
Rock specific heat	C_r	1000 $\frac{J}{kg \cdot K}$
Aquifer length	x	1828 m
Node spacing (x)‡	Δx	304.666
Aquifer width	y	182.8 m
Node spacing (y)‡	Δy	30.4666
Reference temperature	T	250°C
Initial pressure	P_0	4.3 MPa
Initial water saturation	S_{l0}	0.2
Residual liquid saturation	S_{lr}	0.05
Residual vapor saturation	S_{lv}	0.05
Capillary pressure at zero saturation	P_{capmax}	1.0 MPa
Saturation at which capillary pressure goes to zero	S_{lmax}	1.0
Aquifer discharge	q_m	0.5 $\frac{kg}{m \cdot s}$
Initial pressure	P_0	4.4816 MPa
Time step	Δt	10 days
Total elapsed time	t	78.31 days

Boundary conditions: At x = 1066.33333, y = 106.63333 q_m = 0.5 $\frac{kg}{m \cdot s}$

No flow across peripheral boundaries

‡ For the FEHM simulation, node spacing around the periphery is half the general spacing to facillitate comparison with Thomas and Pierson who used cell-centered elements, whereas FEHM uses node-centered elements.

4.9.4 Summary of test cases

4.9.4.1 Toronyi two-phase problem

4.9.4.1.1 Function Tested. This test verifies that FEHM has correctly implemented heat and mass transfer and phase partitioning.

4.9.4.1.2 Test Scope. This test case is a verification test.

4.9.4.1.3 Requirements Tested. Requirements 3.1, "Finite-element Coefficient Generation," 3.2, "Formulate Transient Equations" (specifically Sections 3.2.2 and 3.2.6), 3.3, "Apply Constitutive Relationships" (specifically Section 3.3.1), 3.4, "Compute Solution to Transient Equations," and 3.5, "Provide Input/ Output Data Files," of Chapter I are verified by this test.

4.9.4.1.4 Required Inputs. Problem input is provided in the following file:

- *toronyi.in*: basic input and geometry data (64 nodes, 49 elements).

4.9.4.1.5 Expected Outputs. Values from FEHM, for saturation at each interior node at time t = 78.31 days, will be output and compared to the Thomas and Pierson (1978) saturation data. Values within 5% of the Thomas and Pierson solution will be considered acceptable.

DRAFT 4/97

4.10 Test of DOE Code Comparison Project, Problem Five, Case A

4.10.1 Purpose

This model of a 2-D areal reservoir with multiphase flow was developed as part of the DOE Code Comparison Project (Molloy 1980). The two-phase (water/water vapor), heat- and mass-transfer problem is characterized by a moving two-phase boundary. The modeled region has a cold fluid boundary that provides fluid to the system as discharge occurs through a well. Numerical difficulties can occur as nodes go from two-phase to compressed water. This problem is a good test for the two-phase routines, as well as the phase-change algorithm. In addition, this problem provides a test of the code restart capabilities as the initial temperature field is input through use of a restart file. There is no analytical solution for this problem, but results from other codes (Pritchett 1980) are available as a check for FEHM.

4.10.2 Functional description

The test suite consists of a simulation of fluid discharge from a two-phase, 2-D aquifer. Fluid produced at the production well is replaced by cold-water recharge over the length of one of the lateral boundaries. In addition to demonstrating that the heat- and mass-transfer problem has been correctly formulated, the test suite will demonstrate that phase partitioning has been correctly implemented.

4.10.3 Assumptions and limitations

Fluid is discharged from the two-phase geothermal reservoir whereas cold-water recharge occurs over one lateral boundary. The other three boundaries are considered to be impermable and nonconductive. The geometry and boundary conditions are shown in Fig. 11. Of particular note is the variable initial-temperature field and the prescribed pressure and temperature boundary. Table 30 lists the input parameters for the DOE Code Comparison Project problem. A Corey-type relative permeability function is used for this model (see Zyvoloski 1997a, “Relative Permeability and Capillary Pressure Functions” in Section 8.4.3). The reader is referred to Pritchett (1980) for a more detailed discussion of this problem and the code comparison. The solution is verified by comparison of FEHM results to other codes (obtained from Pritchett).

4.10.4 Summary of test cases

4.10.4.1 DOE Code Comparison Project, Problem Five

4.10.4.1.1 Function Tested. This test verifies that FEHM has correctly implemented heat and mass transfer and phase partitioning.

4.10.4.1.2 Test Scope. This test case is a verification test.

4.10.4.1.3 Requirements Tested. Requirements 3.1, “Finite-element Coefficient Generation,” 3.2, “Formulate Transient Equations” (specifically Sections 3.2.2 and 3.2.6), 3.3, “Apply Constitutive Relationships” (specifically Section 3.3.1), 3.4, “Compute Solution to Transient Equations,” 3.5, “Provide Input/Output Data Files,” and 3.6, “Provide Restart Capability” (specifically Sections 3.6.2 and 3.6.3), of Chapter I are verified by this test.

DRAFT 4/97

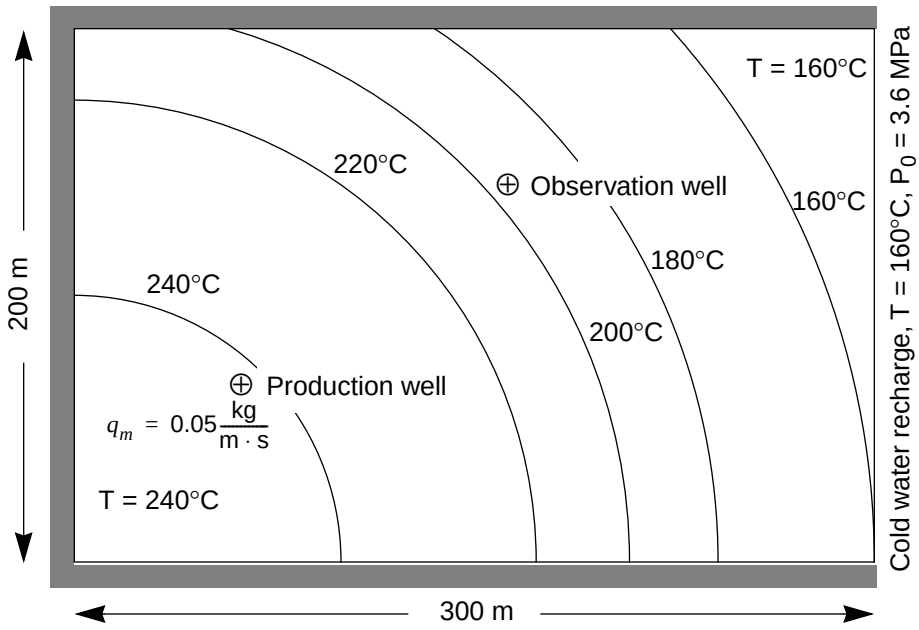

Figure 11. Schematic diagram of the geometry and boundary conditions for the DOE Code Comparison Project problem.

4.10.4.1.4 Required Inputs. Problem input is provided in the following files:

- *doe.dat*: basic input and geometry data (140 nodes, 117 elements) and
- *doe.ini*: initial temperature field, pressure, and saturation.

4.10.4.1.5 Expected Outputs. Values from FEHM for production-well temperature and pressure and pressure at the observation well versus time will be output and compared to the data from other codes. Values within 5% of those obtained by the other codes will be considered acceptable.

DRAFT 4/97

Table 30. Input parameters for the DOE Code Comparison Project, Problem 5, Case A

Parameter	Symbol	Value
Reservoir permeability	k	2.5 x 10^{-14} m^2
Reservoir porosity	ϕ	0.35
Rock thermal conductivity	κ_r	1 $\frac{W}{m \cdot K}$
Rock density	ρ_r	2563 kg/m^3
Rock specific heat	C_r	1010 $\frac{J}{kg \cdot K}$
Reservoir length	x	300 m
Reservoir thickness	y	200 m
Node spacing‡	$\Delta x, \Delta y$	25 m
Liquid residual saturation	S_{lr}	0.3
Gas residual saturation	S_{vr}	0.1
Reservoir discharge	q_m	0.05 $\frac{kg}{m \cdot s}$
Initial pressure	P_0	3.6 MPa
Time step	Δt	30 - 60 days
Total elapsed time	t	10 years

Production-well coordinates: x = 62.5 m, y = 62.5 m
Observation-well coordinates: x = 162.5 m, y = 137.5 m

Initial temperature distribution: [T in °C, r in m ($r = \sqrt{x^2 + y^2}$)]:

$$T(x, y, 0) = \begin{cases} 240 & 0 \le r \\ 240 - 160\left(\frac{r - 100}{200}\right)^2 + 80\left(\frac{r - 100}{200}\right)^4 & 100 < r < 300 \\ 160 & r \ge 300 \end{cases}$$

Boundary conditions: At x = 62.5 m , y = 62.5 m q_m = 0.5 $\frac{kg}{m \cdot s}$
At x = 300m, y = 0 - 200 m T = 160°C, P = P_0 = 3.6 MPa
At x =0 m, y = 0 m, y = 200m Impermable, non-conductive

‡ For the FEHM simulation, node spacing around the periphery is half the general spacing (12.5 m).

DRAFT 4/97

4.11 Test of Dry-out of a Partially Saturated Medium

4.11.1 Purpose

Calculations of fluid flow in the presence of repository heat require the simultaneous solution of a heat- and mass-transfer system consisting of water, water vapor, and air. This test case exercises the code option that solves this type of flow and heat-transport problem by passing air through a one-dimensional, partially saturated medium. The air evaporates water and removes it from the system. A dry-out zone progresses from the injection region through the flow path at a rate that can be predicted using an analytical solution.

4.11.2 Functional description

The test suite consists of a simulation of the rate of movement of a dry region, starting at a condition of constant saturation throughout the flow path. Two cases are considered: a system without vapor-pressure lowering and one with vapor-pressure lowering, which lowers the water-vapor carrying capacity of the injected air.

4.11.3 Assumptions and limitations

If dry air is injected into a partially saturated medium containing immobile liquid water, the water evaporates until the partial pressure of water vapor in the gas reaches its equilibrium vapor pressure. For a mass flow rate of air of $\dot{m}_a$ and assuming ideal-gas-mixture conditions, the corresponding rate of removal of water in the gas $\dot{m}_w$ is given by

$$\dot{m}_w = \frac{M_w P_w \dot{m}_a}{M_a P_a} ,$$

where M_w and M_a are molecular weights and P_w and P_a are partial pressures with the subscripts w and a referring to the water and air, respectively. Assuming that the dry-out occurs as a sharp front, the rate of progression of this front can be shown to be

$$r_{dry} = \frac{L\dot{m}_a M_w P_w}{\phi S V \rho_w M_a P_a} .$$

In this equation, L is the flow path length, V is the volume, and S is the liquid saturation. The problem is depicted in Fig. 12. Table 31 lists the input parameters used in this comparison. When vapor-pressure lowering is included, the value of P_w in the equation is lower than it would be in the absence of this effect. The capillary pressure in these simulations is adjusted so that it is a constant value throughout the column, regardless of saturation. Its value is set using the linear capillary-pressure model such that the water vapor pressure is lowered by a factor of 2.

DRAFT 4/97

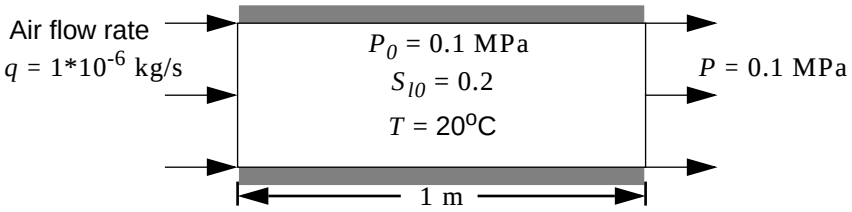

Figure 12. Schematic drawing of the geometry and boundary conditions for the dry-out simulations.

Table 31. Input parameters for the dry-out simulations

Parameter	Symbol	Value
Air flow rate	q	1.0*10^{-6} kg/s
Volume of path	V	1 m^3
Length of path	L	1 m
Node spacing	Δl	0.005 m
Porosity	ϕ	0.05
Time step w/o vapor-pressure lowering with vapor-pressure lowering	Δt	 0.001 - 1.5 days 0.001 - 3 days
Total elapsed time w/o vapor-pressure lowering with vapor-pressure lowering	t	 500 days 1000 days
Total system pressure	P_0	0.1 MPa
Temperature (from which P_w is computed)	T	20°C
Initial water saturation	S_{l0}	0.2
Residual liquid saturation	S_{lr}	0.3
Residual vapor saturation	S_{lv}	0.3
Maximum liquid saturation	S_{lmax}	1.0
Maximum vapor saturation	S_{vmax}	1.0
Boundary conditions: At l = 0 At l = 1		q = 1*10^{-6} kg/s P = 0.1 MPa

DRAFT 4/97

4.11.4 Summary of test cases

4.11.4.1 Dry-out without vapor-pressure lowering

4.11.4.1.1 Function Tested. This test verifies that FEHM correctly simulates the dry-out of a partially saturated medium in the absence of vapor-pressure lowering.

4.11.4.1.2 Test Scope. This test case is a verification test.

4.11.4.1.3 Requirements Tested. Requirements 3.1, "Finite-element Coefficient Generation," 3.2, "Formulate Transient Equations" (specifically Sections 3.2.3 and 3.2.6), 3.3, "Apply Constitutive Relationships" (specifically Sections 3.3.2 and 3.3.4), 3.4, "Compute Solution to Transient Equations," and 3.5, "Provide Input/Output Data Files," of Chapter I are verified by this test.

4.11.4.1.4 Required Inputs. Problem input is provided in the following files:

- *dryout1.in*: basic input data and
- *dryout.geom*: geometry data (the grid consists of 201 x 2 nodes, thus simulating a one-dimensional flow system).

4.11.4.1.5 Expected Outputs. Values from FEHM for the position of the dry-out front at five different times should agree with the analytical solution. Position within 5% of the predicted value will be considered acceptable.

4.11.4.2 Dry-out with vapor-pressure lowering

4.11.4.2.1 Function Tested. This test verifies that FEHM correctly simulates the dry-out of a partially saturated medium when vapor-pressure lowering is included.

4.11.4.2.2 Test Scope. This test case is a verification test.

4.11.4.2.3 Requirements Tested. Requirements 3.1, "Finite-element Coefficient Generation," 3.2, "Formulate Transient Equations" (specifically Sections 3.2.3 and 3.2.6), 3.3, "Apply Constitutive Relationships" (specifically Sections 3.3.2 and 3.3.4), 3.4, "Compute Solution to Transient Equations," and 3.5, "Provide Input/Output Data Files," of Chapter I are verified by this test.

4.11.4.2.4 Required Inputs. Problem input is provided in the following files:

- *dryout2.in*: basic input data and
- *dryout.geom*: geometry data (the grid consists of 201 x 2 nodes, thus simulating a one-dimensional flow system).

4.11.4.2.5 Expected Outputs. Values from FEHM for the position of the dry-out front at five different times should agree with the analytical solution. Position within 5% of the predicted value will be considered acceptable.

DRAFT 4/97

4.12 Test of One-dimensional Reactive-solute Transport

4.12.1 Purpose

Tracers are used extensively to determine travel times and reservoir volumes. Reactive tracers can be used to infer reservoir properties such as temperature and geochemical composition. Reactive tracers will be used in the C-wells testing at Yucca Mountain. Of course, solute transport capabilities are also used to simulate radionuclide migration. A YMP code, SORBEQ (Robinson 1993), has been developed and validated to model one-dimensional reactive-solute flow and adsorption. FEHM will be compared with SORBEQ on a one-dimensional solute problem with equilibrium sorption. This comparison will verify the species transport in one dimension, and because the codes use different numerical techniques (finite differences versus finite elements), this test suite provides an independent check of both codes.

4.12.2 Functional Description

The test suite consists of a simulation of solute transport for five independent species: a conservative solute and species governed by the linear, Langmuir, Freundlich, and modified Fruendlich isotherms.

4.12.3 Assumptions and limitations

The problem is depicted in Fig. 13. Table 32 defines the input parameters used for FEHM and SORBEQ simulations. The adsorption parameters are given in Table 33. A fluid-flow steady state is established by injecting fluid at a fixed flow rate at the inlet and applying a constant-pressure boundary condition at the outlet. The solute transport simulation is executed assuming an initial concentration of zero everywhere in the column and injecting fluid with a concentration of unity at the start of the solute transport phase of the simulation. For each solute, the same dispersivity is assumed (0.033 m, equivalent to a dimensionless Peclet number L/α of 30). The inlet concentration remains at unity for the entire simulation.

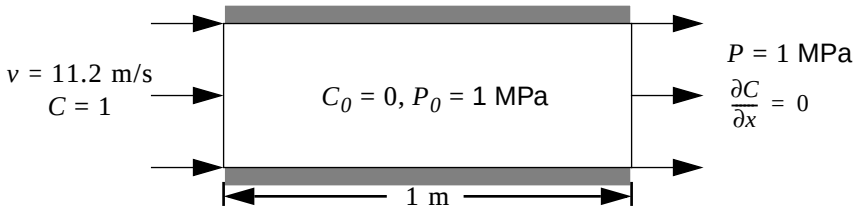

Figure 13. Schematic drawing of the geometry and boundary conditions for the 1-D reactive-tracer transport problem.

DRAFT 4/97

Table 32. Input parameters for the 1-D reactive-tracer transport problem

Parameter	Symbol	Value
Fluid velocity	v	11.2 m/s
Flow path length	L	1 m
Node spacing	Δl	0.005 m
Dispersivity	α	0.033 m
Porosity	ϕ	0.3
Bulk-rock density	ρ_b	2500 kg/m^3
Time step (tracer)	Δt	0.09 - 0.43 s
Total elapsed time	t	100 s
Pressure	P_0	1.0 MPa
Initial concentration	C_0	0.0
Inlet concentration	C_{in}	1
Boundary conditions: At l = 0	C = 1	
At l = 1	P = 1 MPa, $\frac{\partial C}{\partial x} = 0$	

Table 33. Adsorption parameters for the reactive-tracer transport problem

Adsorption isotherm	α_1	α_2	β
Conservative	0.0	0.0	1.0
Linear	0.25	0.0	1.0
Langmuir	0.24	1.0	1.0
Freundlich	0.12	0.0	0.8
Modified Freundlich	0.48	1.0	0.8

4.12.4 Summary of test cases

4.12.4.1 Reactive-tracer transport

4.12.4.1.1 Function Tested. This test verifies that FEHM has correctly implemented reactive-tracer transport.

4.12.4.1.2 Test Scope. This test case is a verification test.

4.12.4.1.3 Requirements Tested. Requirements 3.1, “Finite-element Coefficient Generation,” 3.2, “Formulate Transient Equations”

(specifically Sections 3.2.4 and 3.2.6), 3.3, "Apply Constitutive Relationships" (specifically Section 3.3.5), 3.4, "Compute Solution to Transient Equations," and 3.5, "Provide Input/ Output Data Files," of Chapter I are verified by this test.

4.12.4.1.4 Required Inputs. Problem input is provided in the following file:

- *sorption.in*: basic input and geometry data (402 nodes, 200 elements). A single simulation is performed that contains five noninteracting solutes with sorption parameters defined in Table 33.

4.12.4.1.5 Expected Outputs. Breakthrough curves (concentration at the outlet node for each species versus time) from FEHM will be output and compared to the SORBEQ solutions. When concentrations are close to zero, percent errors are misleading. Furthermore, considerable concentration errors result from only a small displacement of a breakthrough curve along the time axis because of the steep rise of the concentration-time curve for a typical case. Therefore, concentrations within 0.01 of the SORBEQ solutions and percent errors less than 10% when concentrations are greater than 0.1 will be considered acceptable.

DRAFT 4/97

4.13 Test of Henry's Law Species

4.13.1 Purpose

This set of verification runs tests the numerous combinations of effects possible for Henry's Law solutes that may sorb or undergo chemical reaction. Two extremes for the one-dimensional flow field are employed: 1) air moving through a stagnant fluid phase and 2) water moving through a stagnant air phase. The solute will partition into the stagnant fluid, resulting in a decrease in the overall solute transport velocity similar to that observed with equilibrium sorption.

4.13.2 Functional description

The problem set has been divided into three segments. Segment 1 covers air moving through a stagnant fluid phase, and Segment 2 covers water moving through a stagnant air phase. Segment 3 contains problems similar to those of Segments 1 and 2 except that chemical reaction is also included for the Henry's Law species. The approach here is to check the results of a Henry's Law species against tests of a liquid- or vapor-only species under conditions designed to give similar breakthrough times. Table 34 outlines the combinations of chemical phenomena exercised in each problem

Table 34. Combinations of phenomena exercised in the tests of Henry's Law species

Problem	Mobile phase	Sorption	Reaction
1-1	air	none	none
1-2	air	liquid-rock	none
1-3	air	vapor-rock	none
2-1	water	none	none
2-2	water	liquid-rock	none
2-3	water	vapor-rock	none
3-1	water	none	liquid and vapor
3-2	water	liquid-rock	liquid and vapor
3-3	air	vapor-rock	liquid and vapor

4.13.3 Assumptions and limitations

Problem 1-1: A Henry's Law constant (K_H) was chosen so that at any location half of the species resides in the vapor and half in the liquid. In the simulation, the tracer is exchanged between the flowing vapor and stagnant liquid. Therefore, this solute should behave identically to a linearly sorbing solute (see verification in the previous section, Section 4.12) with a sorption parameter that yields a velocity of one-half the conservative tracer velocity.

Problem 1-2: A Henry's Law constant of twice that of Problem 1-1, combined with an appropriate liquid-borne solute-rock sorption parameter,

results in a partitioning of the solute of one-half vapor, one-fourth liquid, and one-fourth sorbed from liquid to rock. The results should be virtually identical to those of Problem 1-1, showing that the coupling of liquid to solid sorption is implemented properly for a Henry's Law species.

Problem 1-3: This problem is similar to Problem 1-2 except that sorption occurs from the vapor to the rock. The results should be virtually identical to those of Problem 1-1.

Problems 2-1, 2-2, and 2-3: These runs are similar to their counterparts in Segment 1, except that the water phase is moving. The breakthrough curves should agree closely with that obtained for a liquid-only species undergoing sorption.

Problem 3-1: This problem tests a Henry's Law species with no sorption but with chemical reaction taking place in both the vapor and liquid (implemented as two independent chemical reactions). The steady-state concentration exiting the reactor is compared to that of a liquid-only species that reacts at twice the rate. Because the solute remains in the system twice as long for the Henry's Law species, rate constants lower by a factor of two for both the liquid and vapor should yield the same steady-state concentration as the liquid-only species.

Problem 3-2: This problem is an extension of Problem 3-1 that includes sorption from liquid to rock. Chemical reaction is specified as taking place in the liquid, vapor, and sorbed phase, with rate constants selected so that the results should agree with those of Problem 3-1. Two cases are tested: Henry's Law with sorption and liquid-only with sorption.

Problem 3-3: This problem is the same as Problem 3-2 except that the air is the moving phase and sorption is from vapor to rock.

The problem geometry is depicted in Fig. 14. Table 35 defines the input parameters, and the adsorption, Henry's law, and reaction parameters are given in Table 36. The problems are isothermal.

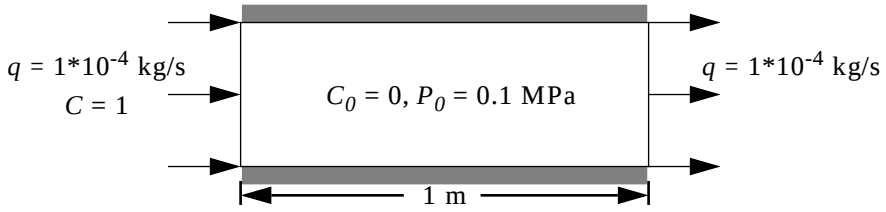

Figure 14. Schematic drawing of the geometry and boundary conditions for the tests of Henry's Law species.

DRAFT 4/97

Table 35. Input parameters for the tests of Henry's Law species

Parameter	Symbol	Value
Fow rate (liquid flow rate for mobile-liquid case, air flow rate for mobile-air case)	q	$1.0*10^{-4}$ kg/s
Flow path length	L	1 m
Node spacing	Δl	0.005 m
Dispersivity	α	0.033 m
Porosity	ϕ	0.05
Permeability	k	
Mobile air phase		$1*10^{-11}$ m^2
Mobile water phase		$1*10^{-12}$ m^2
Bulk-rock density	ρ_b	2500 kg/m^3
Time step (tracer)	Δt	
Mobile air phase		0.09 - 0.43 s
Mobile water phase		500 s
Total elapsed time (tracer)	t	
Mobile air phase		864 s
Mobile water phase		6 days
Pressure	P_0	0.1 MPa
Reference pressure	P_{ref}	0.1 MPa
Reference temperature	T_{ref}	20^oC
Initial water saturation	S_{l0}	
Mobile air phase		0.2
Mobile water phase		0.5
Residual liquid saturation	S_{lr}	
Mobile air phase		0.3
Mobile water phase		0.0
Residual vapor saturation	S_{lv}	
Mobile air phase		0.3
Mobile water phase		0.6
Maximum liquid saturation	S_{lmax}	
Mobile air phase		1.0
Mobile water phase		0.3
Maximum vapor saturation	S_{vmax}	
Mobile air phase		1.0
Mobile water phase		0.0

DRAFT 4/97

Table 35. Input parameters for the tests of Henry's Law species (continued)

Parameter		Symbol	Value
Initial concentration		C_0	0.0
Inlet concentration		C_{in}	1
Boundary conditions:	At l = 0		C = 1, q = 1.0*10^{-4} kg/s
	At l = 1		q = 1.0*10^{-4} kg/s

Table 36. Adsorption, Henry's Law, and reaction parameters for the tests of Henry's Law species

Problem	α_1	α_2	β	K_H	Reaction
1-1 (both phases)	0.0	0.0	1.0	33.64	N/A
1-2				67.24	
vapor phase	0.0	0.0	1.0		N/A
liquid phase	9.4972*10^{-6}	0.0	1.0		
1-3				67.24	
vapor phase	3.991*10^{-3}	0.0	1.0		N/A
liquid phase	0.0	0.0	1.0		
2-1 (both phases)	0.0	0.0	1.0	134.0127	N/A
2-2				67.00635	
vapor phase	0.0	0.0	1.0		N/A
liquid phase	4.989*10^{-3}	0.0	1.0		
2-3				67.00635	
vapor phase	1.191*10^{-5}	0.0	1.0		N/A
liquid phase	0.0	0.0	1.0		
3-1	0.0	0.0	1.0	134.0127	liquid and vapor
3-2				67.00635	liquid,
vapor phase	0.0	0.0	1.0		vapor, and
liquid-phase adsorption	4.989*10^{-3}	0.0	1.0		sorbed
3-3				67.24	liquid,
vapor phase	0.0	0.0	1.0		vapor, and
liquid phase	9.4972*10^{-6}	0.0	1.0		sorbed

DRAFT 4/97

4.13.4 Summary of test cases

4.13.4.1 Air movement through stagnant water

4.13.4.1.1 Function Tested. This test verifies that FEHM correctly simulates the transport of a species that partitions between a mobile air phase and immobile water.

4.13.4.1.2 Test Scope. This test case is a verification test.

4.13.4.1.3 Requirements Tested. Requirements 3.1, "Finite-element Coefficient Generation," 3.2, "Formulate Transient Equations" (specifically Sections 3.2.4 and 3.2.6), 3.3, "Apply Constitutive Relationships" (specifically Section 3.3.5), 3.4, "Compute Solution to Transient Equations," and 3.5, "Provide Input/ Output Data Files," of Chapter I are verified by this test.

4.13.4.1.4 Required Inputs. Problem input is provided in the following files:

- *henry1-1.in*: basic input data,
- *henry1-2.in*: basic input data,
- *henry1-3.in*: basic input data, and
- *henry.geom*: geometry data (this two-dimensional grid contains 201 nodes in the flow direction and 2 in the direction perpendicular to flow, making this effectively a one-dimensional simulation).

4.13.4.1.5 Expected Outputs. Values from FEHM for concentration versus time at the outlet node will be output and compared to the FEHM solution for a linearly sorbing solute with a retardation factor of 2. Concentrations within 0.01 of the sorbing-solute solution and percent errors less than 10% when concentrations are greater than 0.1 will be considered acceptable.

4.13.4.2 Water movement through stagnant air

4.13.4.2.1 Function Tested. This test verifies that FEHM correctly simulates the transport of a species that partitions between a mobile water phase and immobile air.

4.13.4.2.2 Test Scope. This test case is a verification test.

4.13.4.2.3 Requirements Tested. Requirements 3.1, "Finite-element Coefficient Generation," 3.2, "Formulate Transient Equations" (specifically Sections 3.2.4 and 3.2.6), 3.3, "Apply Constitutive Relationships" (specifically Section 3.3.5), 3.4, "Compute Solution to Transient Equations," and 3.5, "Provide Input/ Output Data Files," of Chapter I are verified by this test.

4.13.4.2.4 Required Inputs. Problem input is provided in the following files:

- *henry2-1.in*: basic input data,
- *henry2-2.in*: basic input data,
- *henry2-3.in*: basic input data, and
- *henry.geom*: geometry data.

4.13.4.2.5 Expected Outputs. Values from FEHM for concentration versus time at the outlet node will be output and compared to the FEHM solution for a linearly sorbing solute with a retardation factor of 2. Concentrations within 0.01 of the

sorbing-solute solution and percent errors less than 10% when concentrations are greater than 0.1 will be considered acceptable.

4.13.4.3 Air/water movement through stagnant water/air with chemical reaction

4.13.4.3.1 Function Tested. This test verifies that FEHM correctly simulates the transport of a species that partitions between a mobile air phase and immobile water and for which the solute also undergoes an irreversible, first-order reaction.

4.13.4.3.2 Test Scope. This test case is a verification test.

4.13.4.3.3 Requirements Tested. Requirements 3.1, "Finite-element Coefficient Generation," 3.2, "Formulate Transient Equations" (specifically Sections 3.2.4 and 3.2.6), 3.3, "Apply Constitutive Relationships" (specifically Sections 3.3.5 and 3.3.6), 3.4, "Compute Solution to Transient Equations," and 3.5, "Provide Input/Output Data Files," of Chapter I are verified by this test.

4.13.4.3.4 Required Inputs. Problem input is provided in the following files:

- *henry3-1.in*: basic input data,
- *henry3-2.in*: basic input data,
- *henry3-3.in*: basic input data, and
- *henry.geom*: geometry data.

4.13.4.3.5 Expected Outputs. Values from FEHM for concentration versus time at the outlet node will be output and compared to the FEHM solution for the input file *henry3-1.in* (species 1). Concentrations within 0.01 of the sorbing-solute solution and percent errors less than 10% when concentrations are greater than 0.1 will be considered acceptable. For input files *henry3-1.in* (species 2), *henry3-2.in*, and *henry3-3.in*, only the steady-state concentration at the end of the simulation will be compared to that for a one-dimensional, plug flow (constant velocity) system with reaction. Values within 5% of the plug flow solution will be considered acceptable.

DRAFT 4/97

4.14 Test of Fracture Transport with Matrix Diffusion

4.14.1 Purpose

Matrix diffusion is an important process in the transport of contaminants in fractured porous media. Under certain limiting conditions, analytical solutions have been developed. The transport module of FEHM with equilibrium sorption can be tested in two dimensions against these analytical solutions to ensure that multidimensional transport problems with sorption are properly formulated.

4.14.2 Functional description

The test suite developed here consists of a two-dimensional grid with a permeability field set up to simulate one-dimensional flow in a fracture (a line of nodes along one edge of the model domain). Fluid in the surrounding matrix is stagnant. Tracers injected with the flowing fluid in the fracture can transport into the matrix via molecular diffusion. Sorption can occur either on the fracture, in the matrix, or both. The results for the breakthrough curve (concentration versus time at the outlet of the fracture) can be compared against analytical solutions to test the ability of the code to simulate solute transport with sorption.

4.14.3 Assumptions and limitations

Tang et al. (1981) present an analytical solution for the case of one-dimensional axial dispersion in the fracture coupled to diffusion into an infinite medium (Eqn. 35 in Tang et al. (1981) revised for a fixed observation point a distance L from the inlet and no radioactive decay):

$$\frac{C}{C_{in}} = \frac{2 \cdot \exp\left(\frac{L}{2\alpha}\right)}{\pi^{1/2}} \int_l^{\infty} \exp\left[-\xi^2 - \frac{L^2}{4\alpha^2\xi^2}\right] \operatorname{erfc}\left(\frac{R_f L\tau}{4\alpha A\xi^2}\right) d\xi \ ,$$

where ξ is the integration variable, R_f is the retardation factor on the fracture, and τ is the mean residence time of fluid through the column. The lower integration bound l and the lumped parameter A are given by

$$l = \frac{L}{2}\left(\frac{R_f}{\alpha v t}\right)^{1/2}$$

and

$$A = \frac{bR_f}{\phi(R_m D_{mol})^{1/2}} \ .$$

In the above expressions, v is the fluid velocity, t is time, b is the half-width of the fracture aperture, ϕ is the porosity of the matrix, R_m is the

retardation factor in the matrix, and D_{mol} is the molecular diffusion coefficient of the solute. If we select a molecular diffusion coefficient such that the tracer has insufficient time to diffuse to the edge of the model domain on the opposite side of the fracture, then the solution of Tang et al. should be replicated by FEHM. For sorption, the analytical solution is given in terms of retardation factors for the fracture and matrix. In FEHM, the expression used to duplicate a retardation factor for a saturated medium is

$$R_f = 1 + \frac{\rho_b K_d}{\phi \rho_f},$$

where K_d is the sorption distribution coefficient. The problem geometry (symmetric about the fracture) is depicted in Fig. 15. Table 37 gives the sorption parameters and Table 38 lists the input parameters and conditions for this test suite. Separate cases are run with no sorption, sorption in the matrix, and sorption in both the fracture and matrix (flow occurs only in the fracture).

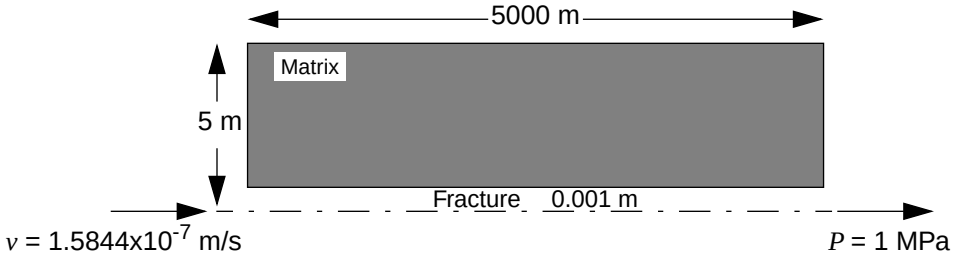

Figure 15. Schematic drawing of the geometry and boundary conditions for the fracture transport problem.

Table 37. Adsorption parameters for the fracture transport problem

Test		α_1	α_2	β
Transport with matrix diffusion, no sorption	fracture	0.0	0.0	1.0
	matrix	0.0	0.0	1.0
Transport with matrix diffusion, sorption (linear) in the matrix	fracture	0.0	0.0	1.0
	matrix	$7.4074(10^{-2})$	0.0	1.0
Transport with matrix diffusion, sorption in the fracture and matrix	fracture	8.88889	0.0	1.0
	matrix	$7.4074(10^{-2})$	0.0	1.0

DRAFT 4/97

Table 38. Input parameters for the test of the matrix-diffusion problem

Parameter	Symbol	Value
Flow path length (x)	L	5000 m
Node spacing along flow path‡	Δx	100 m
Model width	y	5 m
Node spacings	Δy	0.001 - 0.5 m
Fluid density	ρ_f	1000 kg/m^3
Bulk-rock density	ρ_b	2700 kg/m^3
Matrix porosity	ϕ	0.05
Pore-water velocity	v	1.5844x10^{-7} m/s
Dispersivity in fracture	α	500 m
Matrix diffusion coefficient	D_{mol}	1.5x10^{-12} m^2/s
Fracture retardation ractor	R_f	1 or 25
Matrix retardation factor	R_m	1 or 5
Time step (tracer)	Δt	0.001 - 5000 days
Total elapsed time	t	1500 years
Pressure	P_0	1.0 MPa
Initial concentration	C_0	0.0
Inlet concentration	C_{in}	1
Boundary conditions: At l = 0 m	$q = v\rho_f\phi = 7.922 \times 10^{-6}$ kg/s	
At l = 5000 m	P = 1 MPa	

‡The node spacing at each edge is 1 m to accomodate boundary conditions.

4.14.4 Summary of test cases

4.14.4.1 Transport with matrix diffusion, no sorption

4.14.4.1.1 Function Tested. This test verifies that FEHM correctly simulates the transport system consisting of flow and dispersion in a fracture with diffusion into the rock matrix.

4.14.4.1.2 Test Scope. This test case is a verification test.

4.14.4.1.3 Requirements Tested. Requirements 3.1, “Finite-element Coefficient Generation,” 3.2, “Formulate Transient Equations”

(specifically Sections 3.2.4 and 3.2.6), 3.3, "Apply Constitutive Relationships" (specifically Section 3.3.5), 3.4, "Compute Solution to Transient Equations," and 3.5, "Provide Input/ Output Data Files," of Chapter I are verified by this test.

4.14.4.1.4 Required Inputs. Problem input is provided in the following files:

- *tangtest1.in*: basic input data and
- *tangtest.geom*: coordinate and element information. The geometry is represented by a two-dimensional grid of 1590 nodes (53 in the direction of flow and 30 in the matrix). The node spacing in the matrix is small near the fracture where concentration gradients are largest.

4.14.4.1.5 Expected Outputs. Values from FEHM for concentration breakthrough curves will be output and compared to the analytical solution results. A root-mean-square error of the difference between the FEHM and Tang solutions less than or equal to 0.01 for concentrations greater than 0.1 will be considered acceptable.

4.14.4.2 Transport with matrix diffusion, sorption in the matrix

4.14.4.2.1 Function Tested. This test verifies that FEHM correctly simulates the transport system consisting of flow and dispersion in a fracture with diffusion into the rock matrix and with sorption occurring in the matrix.

4.14.4.2.2 Test Scope. This test case is a verification test.

4.14.4.2.3 Requirements Tested. Requirements 3.1, "Finite-element Coefficient Generation," 3.2, "Formulate Transient Equations" (specifically Sections 3.2.4 and 3.2.6), 3.3, "Apply Constitutive Relationships" (specifically Section 3.3.5), 3.4, "Compute Solution to Transient Equations," and 3.5, "Provide Input/ Output Data Files," of Chapter I are verified by this test.

4.14.4.2.4 Required Inputs. Problem input is provided in the following files:

- *tangtest2.in*: basic input data and
- *tangtest.geom*: coordinate and element information. The geometry is represented by a two-dimensional grid of 1590 nodes (53 in the direction of flow and 30 in the matrix). The node spacing in the matrix is small near the fracture where concentration gradients are largest.

4.14.4.2.5 Expected Outputs. Values from FEHM for concentration breakthrough curves will be output and compared to the analytical solution results. A root-mean-square error of the difference between the FEHM and Tang solutions less than or equal to 0.01 for concentrations greater than 0.1 will be considered acceptable.

4.14.4.3 Transport with matrix diffusion and with sorption in the fracture and matrix

4.14.4.3.1 Function Tested. This test verifies that FEHM correctly simulates the transport system consisting of flow and dispersion in a fracture with diffusion into the rock matrix and with sorption occurring in the matrix and on the fracture.

4.14.4.3.2 Test Scope. This test case is a verification test.

4.14.4.3.3 Requirements Tested. Requirements 3.1, "Finite-element Coefficient Generation," 3.2, "Formulate Transient Equations" (specifically Sections 3.2.4 and 3.2.6), 3.3, "Apply Constitutive Relationships" (specifically Section 3.3.5), 3.4, "Compute Solution to Transient Equations," and 3.5, "Provide Input/ Output Data Files," of Chapter I are verified by this test.

4.14.4.3.4 Required Inputs. Problem input is provided in the following files:

- *tangtest3.in*: basic input data and
- *tangtest.geom*: coordinate and element information. The geometry is represented by a two-dimensional grid of 1590 nodes (53 in the direction of flow and 30 in the matrix). The node spacing in the matrix is small near the fracture where concentration gradients are largest.

4.14.4.3.5 Expected Outputs. Values from FEHM for concentration breakthrough curves will be output and compared to the analytical solution results. A root-mean-square error of the difference between the FEHM and Tang solutions less than or equal to 0.01 for concentrations greater than 0.1 will be considered acceptable.

DRAFT 4/97

4.15 Test of the Movement of a Dissolved Mineral Front

4.15.1 Purpose

The ability of FEHM to model precipitation and dissolution reactions allows us to develop more sophisticated models to describe the rock-water interactions at the Yucca Mountain site. The analytical solution for a single, sharp-moving, equilibrium mineral front has been used to verify reactive-transport models in the past (i.e., Engesgaard 1991; Walsh et al. 1984). This analytical solution, which assumes no dispersion, is used to verify that FEHM is accurately predicting the velocity of a dissolved mineral front.

4.15.2 Functional description

A one-dimensional transport simulation of calcite ($CaCO_3(s)$) dissolution is tested. Profiles of concentration versus reactor length, at selected times, will be compared against the analytical solution.

4.15.3 Assumptions and limitations

The precipitation and dissolution of calcite (a common mineral in many soils) are important processes that play a significant role in controlling the pH and alkalinity of groundwater. The dissolution reaction and the solubility product for this problem are

$$CaCO_{3(s)} \Leftrightarrow Ca_{(aq)} + CO_{3(aq)} \quad \text{and} \quad K_{sp} = 3.919x10^{-9}(\text{mol/ kg})^2 \ .$$

Thus, the transport system (illustrated in Fig. 16) consists of one equilibrium reaction with three species.

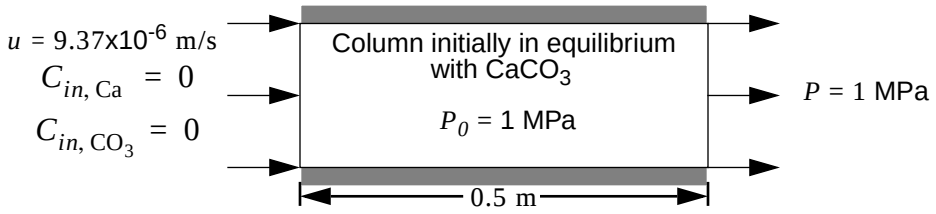

Figure 16. Schematic drawing of the geometry and boundary conditions for the calcite-dissolution problem.

The analytical solution for a single dissolved mineral front (Fig. 17) is given by

$$u_{mineral} = \frac{u\Delta C_{aq}}{\Delta C_{aq} + \frac{\rho_b}{\phi}\Delta C_s} \ ,$$

where u is the pore-water velocity, $u_{mineral}$ is the velocity of the mineral front, ρ_b is the bulk-rock density, ϕ is the porosity, ΔC_s is the change in solid concentration across the front, and ΔC_{aq} is the change in aqueous

concentration across the front. A list of relevant input parameters and conditions is given in Table 39.

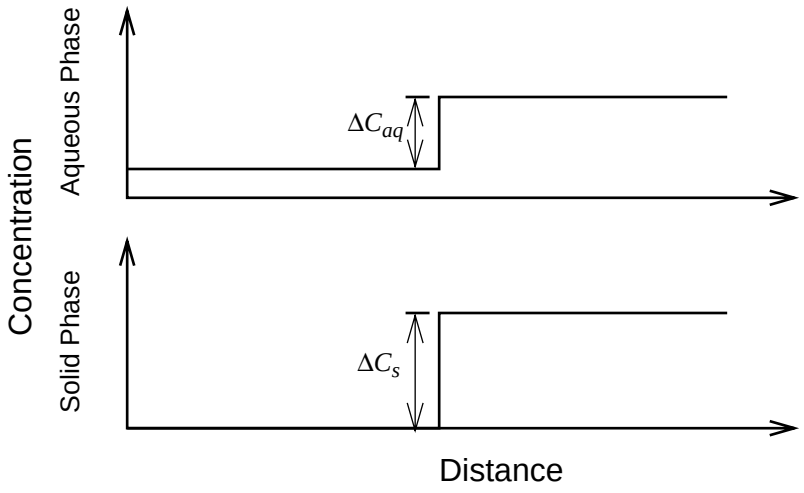

Figure 17. Aqueous and mineral-front profiles modeled by the analytical solution.

4.15.4 Summary of test cases

4.15.4.1 Calcite dissolution in a one-dimensional system

4.15.4.1.1 Function Tested. This test verifies that FEHM correctly simulates the dissolution of a mineral.

4.15.4.1.2 Test Scope. This test case is a verification test.

4.15.4.1.3 Requirements Tested. Requirements 3.1, "Finite-element Coefficient Generation," 3.2, "Formulate Transient Equations" (specifically Section 3.2.4), 3.3, "Apply Constitutive Relationships" (specifically Section 3.3.6), 3.4, "Compute Solution to Transient Equations," and 3.5, "Provide Input/ Output Data Files," of Chapter I are verified by this test.

4.15.4.1.4 Required Inputs. Problem input is provided in the following files:

- *dissolution.in*: basic input data and
- *dissolution.grid*: coordinate and element information (102 nodes, 50 elements to simulate a one-dimensional flow system).

4.15.4.1.5 Expected Outputs. Values from FEHM for the mean concentration of the mineral front will be compared to the analytical solution. Position within 5% of the predicted value will be considered acceptable.

DRAFT 4/97

Table 39. Input parameters for the calcite-dissolution problem

Parameter	Symbol	Value
Reactor length	L	0.5 m
Node spacing	Δl	0.01 m
Fluid density	ρ_f	1000 kg/m^3
Bulk-rock density	ρ_b	1800 kg/m^3
Porosity	ϕ	0.32
Pore-water velocity‡	u	9.37x10^{-6} m/s
Dispersivity	α	0.0067 m
Time step	Δt	100 s
Total elapsed time	t	2.157 days
Pressure	P_0	1.0 MPa
$CaCO_3$ initial concentration	$C_{0,\,CaCO_3}$	2.0x10^{-5} mol/kg-solid
Ca initial concentration	$C_{0,\,Ca}$	6.26x10^{-5} mol/kg-water
CO_3 initial concentration	$C_{0,\,CO_3}$	6.26x10^{-5} mol/kg-water
Ca inlet concentration	$C_{in,\,Ca}$	0
CO_3 inlet concentration	$C_{in,\,CO_3}$	0
Boundary conditions: At l = 0		u = 9.37x10^{-6} m/s $C_{in,\,Ca} = 0$, $C_{in,\,CO_3} = 0$
At l = 1		P = 1 MPa

‡Flow rate $q = u\rho_f\phi/2$ nodes $= 0.0014992$ kg/s

DRAFT 4/97

4.16 Test of Multisolute Transport with Chemical Reaction

4.16.1 Purpose

The coupled transport and chemical reaction of multiple species in solution is an important feature of FEHM that will allow us to incorporate more complex processes into radionuclide transport simulations, as well as to model rock-water interactions at the Yucca Mountain site. The most appropriate way to test this feature of the code is by comparison against a code that was designed specifically for such reactive transport simulations. The code we are using for this purpose is called PDREACT (Valocchi and Pastor 1994), a two-dimensional, isothermal, saturated-zone flow and transport code. This comparison will verify the species transport for a simple, one-dimensional saturated flow field for a complex, multiple-interacting species simulation.

4.16.2 Functional description

The suite of reactions described below are simulated for transport in a one-dimensional flow system. Concentration-versus-time breakthrough curves at the flow path exit and concentration of solid species at the exit versus time will be compared for the two codes.

4.16.3 Assumptions and limitations

The application of this test case is the transport of cobalt (Co) in groundwater. Radioactive cobalt is present in the subsurface at several DOE sites. Although its presence as a divalent cation implies that it should sorb strongly to most soils, its migration rate has been shown to be greater than expected due to complexation with EDTA, a decontaminating agent also found in the subsurface of these sites. Much experimental work has gone into studying the transport of Co as CoEDTA, a much less strongly sorbed species. Figure 18 illustrates the transport problem.

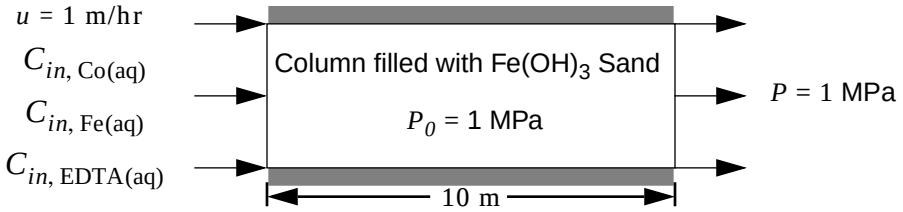

Figure 18. Schematic drawing of the geometry and boundary conditions for the cobalt transport problem.

The chemical reactions and equilibrium or rate constants used to perform this code comparison test are:

$$CoEDTA_{(aq)} \Leftrightarrow Co_{(aq)} + EDTA_{(aq)},\ K_{eq} = 10^{-18}\text{kg/mol};$$

$$Fe_{(aq)} + EDTA_{(aq)} \Leftrightarrow FeEDTA_{(aq)},\ K_{eq} = 6.31\text{x}10^{27}\text{kg/mol};$$

$$Co_{(aq)} \Leftrightarrow Co_{(s)}\ ,\ k_f\ =\ 2.78\text{x}10^{-4}\ \text{s}^{-1},\ k_r\ =\ 5.48\text{x}10^{-5}\ \text{s}^{-1};$$

$$CoEDTA_{(aq)} \Leftrightarrow CoEDTA_{(s)}\ ,\ k_f\ =\ 2.78\text{x}10^{-4}\ \text{s}^{-1},\ k_r\ =\ 5.21\text{x}10^{-4}\ \text{s}^{-1};$$

$$FeEDTA_{(aq)} \Leftrightarrow FeEDTA_{(s)}\ ,\ k_f\ =\ 2.78\text{x}10^{-4}\ \text{s}^{-1},\ k_r\ =\ 6.5\text{x}10^{-4}\ \text{s}^{-1};$$

and

$$CoEDTA_{(s)} + Fe(OH)_{3(s)} \Rightarrow Co_{(s)} + FeEDTA_{(s)},\ k_f\ =\ 3.5x10^{-6}s^{-1}\ .$$

Thus, the transport system consists of 8 species and six reactions, with reactions specified as either equilibrium or kinetically controlled. $Fe(OH)_3$ is so prevalent in the sand that its concentration is assumed to be constant. In addition, this substance does not act as a true species in either simulation. A list of relevant input parameters and conditions for the code comparison are given in Table 40.

4.16.4 Summary of test cases

4.16.4.1 Cobalt transport in a one-dimensional flow system

4.16.4.1.1 Function Tested. This test verifies that FEHM correctly simulates the reactive transport system consisting of both kinetic and equilibrium reactions and with both immobile and aqueous species.

4.16.4.1.2 Test Scope. This test case is a verification test.

4.16.4.1.3 Requirements Tested. Requirements 3.1, “Finite-element Coefficient Generation,” 3.2, “Formulate Transient Equations” (specifically Sections 3.2.4 and 3.2.6), 3.3, “Apply Constitutive Relationships” (specifically Section 3.3.6), 3.4, “Compute Solution to Transient Equations,” and 3.5, “Provide Input/ Output Data Files,” of Chapter I are verified by this test.

4.16.4.1.4 Required Inputs. Problem input is provided in the following file:

- *multi_solute.in*: basic input data, including the finite-element grid with 202 nodes, 100 elements (51 x 2 nodes to simulate a one-dimensional flow system).

4.16.4.1.5 Expected Outputs. Values from FEHM for concentration breakthrough curves of aqueous species and concentration-time history at the outlet node for immobile (solid) species will be output and compared to the PDREACT results. Due to the low inlet concentrations, concentrations within 10% for all values that are greater than 10% of the peak value will be considered acceptable.

DRAFT 4/97

Table 40. Input parameters for test of the reactive transport problem

Parameter	Symbol	Value
Reactor length	L	10 m
Node spacing	Δl	0.1 m
Fluid density	ρ_f	1000 kg/m^3
Bulk-rock density	ρ_b	1500 kg/m^3
Porosity	ϕ	0.4
Pore-water velocity	u	1 m/hr
Dispersivity	α	0.05 m
Time step (tracer)	Δt	0.09 - 360 s
Total elapsed time	t	7.25 days
Pressure	P_0	1.0 MPa
Co inlet concentration	$C_{in,\,\mathrm{Co}}$	3.1623x10^{-5} M
Fe inlet concentration	$C_{in,\,\mathrm{Fe}}$	0 M
EDTA inlet concentration	$C_{in,\,\mathrm{EDTA}}$	3.1623x10^{-5} M
Boundary conditions: At l = 0	u = 1 m/hr	
At l = 1	P = 1 MPa	
‡Flow rate $q = u\rho_f\phi/2$ nodes = 0.05556 kg/s		

DRAFT 4/97

4.17 Test of Three-dimensional Radionuclide Transport

4.17.1 Purpose

A comparison will be made with TRACRN (Travis and Birdsell 1988), another YMP code, on a three-dimensional, single-phase liquid problem. The problem simulates the transport of a tracer undergoing radioactive decay and thus is of particular interest to the Yucca Mountain Project. This comparison will verify the species transport in three dimensions. TRACRN has been compared against many known analytical solutions. Although no three-dimensional analytical solutions exist, a match between TRACRN and FEHM will give confidence that both are correct. Because the codes use different numerical techniques, the test provides a check for both codes.

4.17.2 Functional description

The transport system described below consists of one aqueous species undergoing radioactive decay. Concentration-time histories at several locations in the model domain will be used to make the comparison.

4.17.3 Assumptions and limitations

The radionuclide being simulated is Americium (^{243}Am), which has a half-life of 432 years. The model domain, depicted in Figure 19, is a cube (100 m on each side). Infiltration at a rate of 10^{-4} kg/s occurs over a 100 m^2 region (four nodes) on the top of the box, and outflow is allowed over a 900 m^2 region (36 nodes) on the bottom. The inlet and outlet nodes are offset from each other in plan view so that flow will travel diagonally through the model domain. There is no flow on the remainder of the boundaries. The simulation is run in two parts. After a steady-state flow field is established, a restart run that solves the transport of the radionuclide is carried out. The ^{243}Am is injected with the inlet fluid at a concentration of 1 M. A conservative tracer is also injected with the inlet fluid as an additional check between the two codes. The problem is isothermal. Table 41 lists the input parameters and conditions for this test suite.

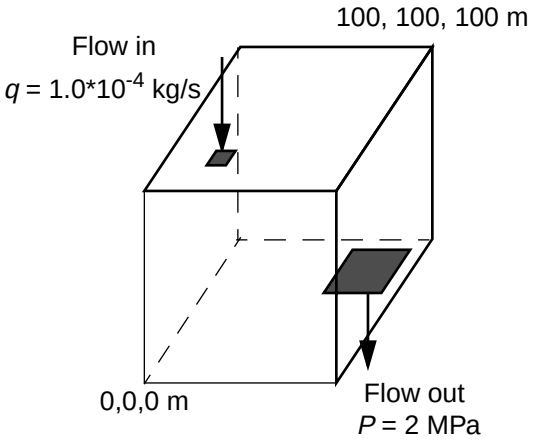

Figure 19. Model domain and flow boundary conditions for test of the radionuclide transport problem.

DRAFT 4/97

Table 41. Input parameters and conditions for test of the radionuclide transport problem

Parameter	Symbol	Value
Reservoir dimensions	x, y, z	100 m
Node spacing‡	$\Delta x, \Delta y, \Delta z$	5 m
Bulk-rock density	ρ_b	2700 kg/m^3
Porosity	ϕ	0.3
Infiltration rate	q	1.0*10^{-4} kg/s
Dispersivity	α	5.0 m
Time step (tracer)	Δt	2.74 - 10 years
Total elapsed time (tracer simulation)	t	5000 years
Pressure	P_0	1.0 MPa
Reference pressure	P_{ref}	0.1 MPa
Reference temperature	T_{ref}	20^{o}C
Initial water saturation	S_{l0}	1.0
Residual liquid saturation	S_{lr}	0.277
Maximum liquid saturation	S_{lmax}	1.0
van Genuchten model parameters		
Inverse of air entry pressure	α_G	3.34 m^{-1}
Power in formula	n	1.982
^{243}Am inlet concentration	$C_{in,\,^{243}\mathrm{Am}}$	1 M
Conservative tracer inlet concentration	$C_{in,\,\mathrm{Cons}}$	1 M

Boundary conditions:
At x = 20 - 30 m, y = 20 - 30 m, z = 100 m: q = 1.0*10^{-4} kg/s
At x = 60 - 90 m, y = 60 - 90 m, z = 0 m: P = 2 MPa

‡ For the FEHM simulation, node spacing around the periphery is half the general spacing (2.5 m).

DRAFT 4/97

4.17.4 Summary of test cases

4.17.4.1 Decay-chain transport in a three-dimensional system

4.17.4.1.1 Function Tested. This test verifies that FEHM correctly simulates the reactive transport system consisting of a radionuclide decay in a three-dimensional flow system. A conservative tracer is also used to verify the three-dimensional tracer transport. In addition, the restart capabilities of the code are verified.

4.17.4.1.2 Test Scope. This test case is a verification test.

4.17.4.1.3 Requirements Tested. Requirements 3.1, "Finite-element Coefficient Generation," 3.2, "Formulate Transient Equations" (specifically Sections 3.2.4 and 3.2.6), 3.3, "Apply Constitutive Relationships" (specifically Section 3.3.5), 3.4, "Compute Solution to Transient Equations," 3.5, "Provide Input/Output Data Files," and 3.6, "Provide Restart Capability," of Chapter I are verified by this test.

4.17.4.1.4 Required Inputs. Problem input is provided in the following files:

- *3d_trac.gen_ini.dat*: basic input data for generating restart and coefficient storage files for the steady-state flow field,
- *3d_trac.grid*: finite-element grid, a structured, three-dimensional grid with 10,648 nodes (22x22x22) and 9261 elements,
- *3d_trac.dat*: basic input data for transport portion of test run,
- *3d_trac.ini*: steady-state flow initialization file (generated during first portion of test run), and
- *3d_trac.stor*: coefficient storage file (generated during first portion of test run).

4.17.4.1.5 Expected Outputs. Values from FEHM for concentration-time histories at specified nodes will be compared to the TRACRN results. A root-mean-square error between FEHM and TRACRN concentrations less than or equal to 0.05, at concentrations greater than 10% of the peak value, will be considered acceptable.

DRAFT 4/97